Electronic Supplemental Information for:

Upcycling natural Limestone waste for thermochemical energy storage by utilising tailored $CaZrO_3$nanoadditives

Rehan Anwar,[a] Jan Navrátil,[b,c] Rajani K. Vijayaraghavan,[d] Patrick J. McNally,[d] Michal Otyepka,[c,e] Piotr Błoński,[c] M. Veronica Sofianos[a*]

[a]School of Chemical and Bioprocess Engineering, University College Dublin, Belfield, Dublin 4, Ireland

[b]Regional Centre of Advanced Technologies and Materials, Czech Advanced Technology and Research Institute (CATRIN), Palacký University, Šlechtitelů 27, 783 71, Olomouc, Czech Republic

[c]Department of Physical Chemistry, Faculty of Science, Palacký University, 17. listopadu 1192/12, 779 00 Olomouc, Czech Republic

[d]School of Electronic Engineering, Dublin City University, Glasnevin, Dublin 9, Ireland

[e]IT4Innovations, Technical University of Ostrava, 708 00 Ostrava-Poruba, Czech Republic

E-mail: mvsofianou@gmail.com

Section S1: Experimental results

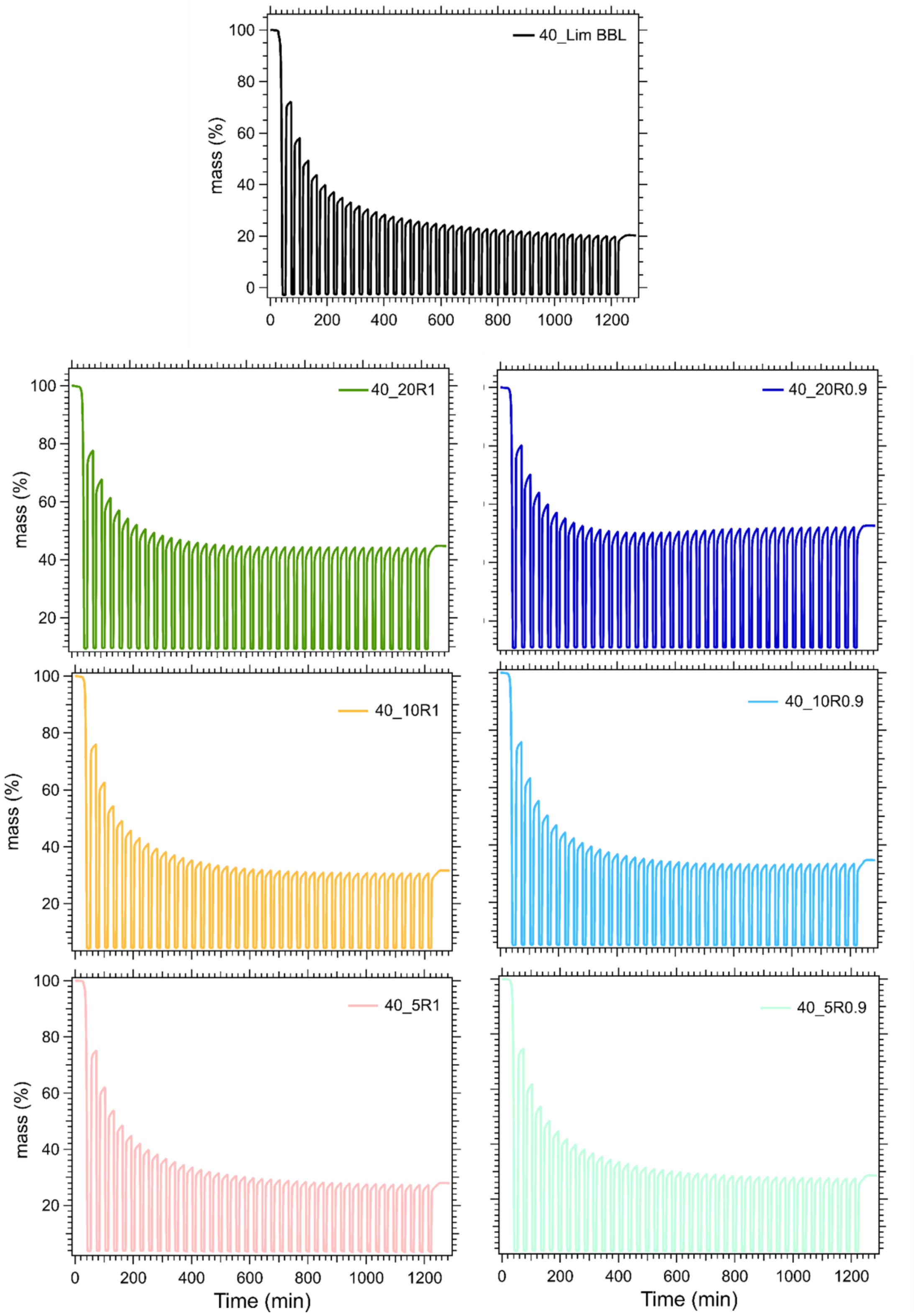

Figure S1. Mass changes of samples *vs* time for 40 cycles (a) Lim BBL (b)20R1 (c) 20R0.9 (d) 10R1 (e) 10R0.9 (f) 5R1 (g) 5R0.9

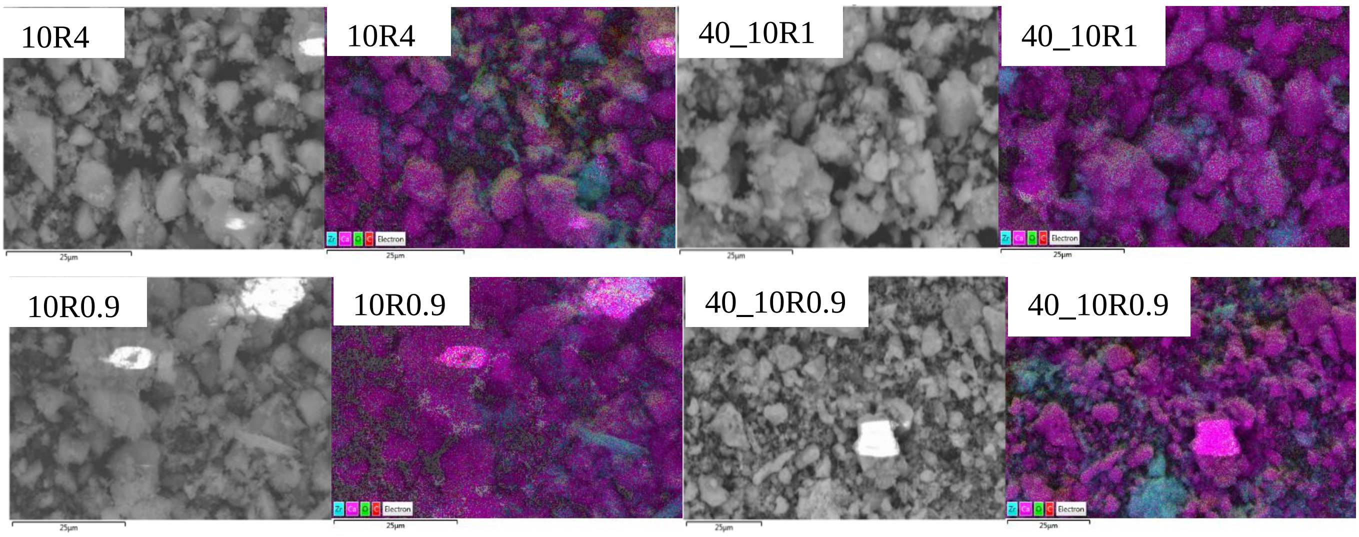

Figure S2. EDS mapping of 10% $CaZrO_3$ samples, before and after 40 cycles

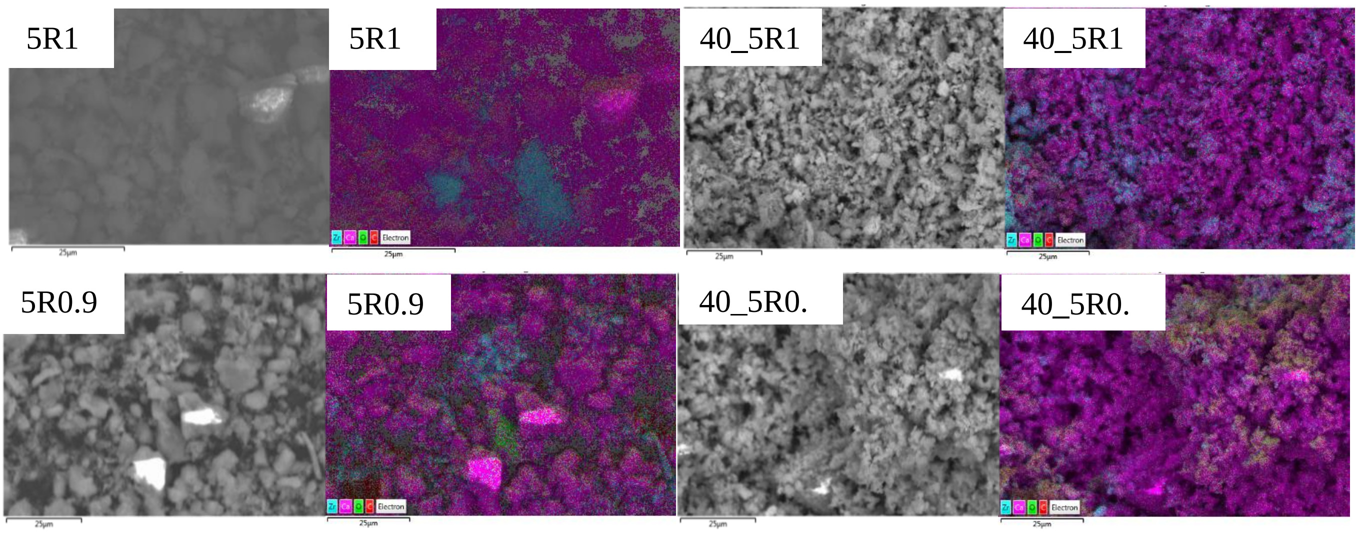

Figure S3. EDS mapping of 5% $CaZrO_3$ samples, before and after 40 cycles

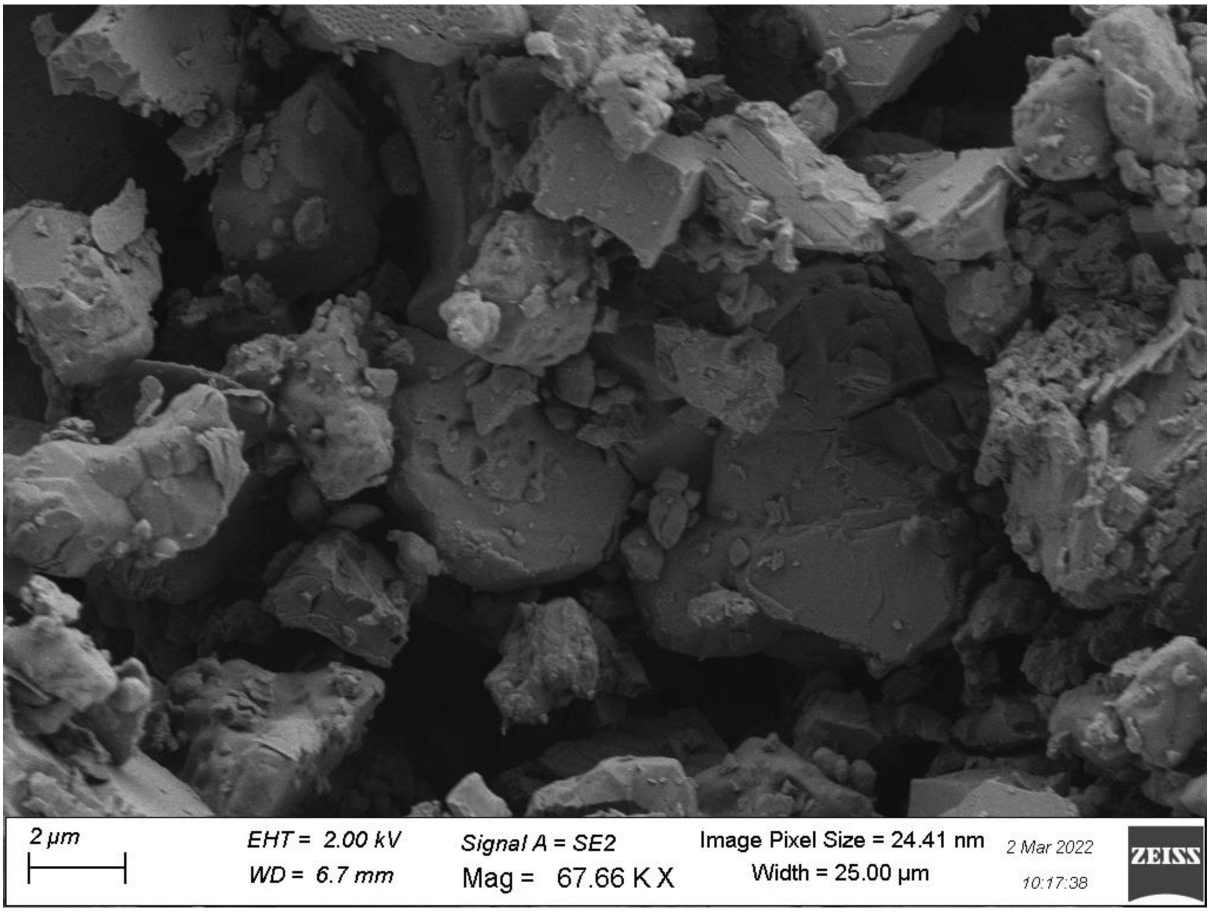

Fig. S4: SEM micrograph of the as-recieved Limestone waste.

Section S2: Computational details

Table S1. Convergence tests of lattice constants with respect to a *k*-point mesh. The relative error is calculated with respect to the lattice constant computed with a 6×6×6 *k*-point mesh

k-point mesh	1×1×1	2×2×2	4×4×4	6×6×6
Lattice constant (Å)	4.2099	4.0344	4.0277	4.0272
Relative error (%)	4.54	0.18	0.01	0.00

Defect formation energy (E_{df}) is calculated from the total energy of the defective system, of the corresponding ideal system, and of the reference systems (RS)

$$E_{df} = E_{tot,def.} - E_{tot,ideal.} - \sum_{RS} N_{RS} \cdot E_{tot,RS}$$

RS is calculated based on

- O ($E_{tot,\mathrm{O}}$) in O_2 molecule in vacuum, $E_{tot,O} = ½ \cdot E_{tot,O_2}$
- Ca ($E_{tot,\mathrm{Ca}}$) in cubic CaO, where the energy of Ca is approximated as $E_{tot,\mathrm{CaO}}$ - $E_{tot,\mathrm{O}}$
- Zr ($E_{tot,\mathrm{Zr}}$) in monoclinic ZrO_2, where the energy of Zr is approximated as $E_{tot,\mathrm{ZrO_2}} - 2 \cdot E_{tot,O}$

Relative energy (E_r) to the structural ground state (GS) in systems with the same element stoichiometry is defined as:

$$E_r = E_{tot} - \min(E_{tot,same})$$

Surface energy (E_s) is calculated following the procedure from Ref. [1]. (001), (110), and (111) surfaces of $CaZrO_3$ were considered. The initial bulk crystal was fully relaxed including basis vectors. Crystal cleavage leads in the case of (001) and (111) surfaces to ZrO_2 termination and CaO termination, thus it is necessary to create two different surface models.

The surface area (S) is given as the vector product of the basis vectors x and y.

E_s has two main contributions: **the cleavage energy** ($E_{s,c}$) and **the relaxation energy** ($E_{s,r}$). The former is mainly attributed to breaking the bonds in the crystal. It is calculated from the total energies of unrelaxed slabs

$$E_{s,c} = \frac{E_{tot,slab1,unrelaxed} + E_{tot,slab2,unrelaxed} - n \cdot E_{tot,bulk}}{4} \cdot \frac{1}{S}$$

where n is

$$n = \frac{N_{atoms,slab1} + N_{atoms,slab2}}{N_{atoms,bulk}}$$

and the factor of 4 accounts for a creation of four new surfaces after two cleavages to make two slabs.

The relaxation energy is attributed to the relaxation of atomic planes after the crystal cleavage. It is calculated as the difference between the total energies of the relaxed and unrelaxed slab resulting in a negative value

$$E_{s,r} = \left(E_{tot,slab,relaxed} - E_{tot,slab,unrelaxed}\right) \cdot \frac{1}{S}$$

The surface energy is calculated as a sum of the two above energies

$$E_s = E_{s,c} + E_{s,r}$$

Section S3: DFT results – Defects in $CaZrO_3$

Table S2. Single-defect formation energy (E_{df}) in bulk $CaZrO_3$ in eV. Ca (Zr) excess means one additional atom at the interstitial position. O → Ca (Zr) means that one O atom is substituted by one Ca or Zr atom. The basic 1×1×1 supercell[1] is $Ca_4Zr_4O_{12}$

	Relaxed lattice					Fixed lattice				
Number of basic cells	1	2	4	6	8	1	2	4	6	8
O vacancy	6.8	6.8	6.9	6.9	8.0	6.8	6.8	6.8	6.9	7.7
Ca vacancy	3.4	3.5	3.6	3.7	3.9	3.3	3.6	3.6	3.6	3.9
Zr vacancy	5.9	6.3	6.5	6.6	6.5	6.0	6.5	6.5	6.4	6.5
Ca excess	11.0	11.3	11.4	11.2	12.5	11.4	11.6	11.6	11.4	12.9
Zr excess	16.7	16.9	16.9	17.0	18.1	17.1	17.1	17.1	17.2	18.7
O → Ca	16.6	18.0	17.3	17.5	18.4	17.2	17.5	17.5	17.6	18.9
O → Zr	21.6	22.8	22.3	22.4	23.2	22.9	22.8	22.5	22.6	23.7

Table S3. Energetics of multiple defects formed in the $Ca_{12}Zr_{12}O_{36}$ supercell. N is the total number of missing atoms and E_{df}/N is the defect formation energy per missing atom. All energies are in eV. Two sets of calculations were performed: one for the lattice with relaxed basis vectors (Relaxed lattice), second for the lattice corresponding to the ideal bulk material (Fixed lattice). The $_{\_n}$ (n = 1, …, 4) subscripts are used to identified structures in figures shown below the table. $Ca_{12}Zr_{12}O_{28}$ and $Ca_{11}Zr_{12}O_{26}$ correspond to the stoichiometries of the experimental samples, $CaZrO_3$-I and $CaZrO_3$-II, respectively

System	N	Relaxed lattice			Fixed lattice		
		E_r	E_{df}	E_{df}/N	E_r	E_{df}	E_{df}/N
$Ca_{12}Zr_{11}O_{28\_1}$	9	0.0	41.2	4.6	0.0	41.1	4.6
$Ca_{12}Zr_{11}O_{28\_2}$	9	1.3	42.5	4.7	0.8	41.9	4.7
$Ca_{12}Zr_{11}O_{28\_3}$	9	1.8	43.0	4.8	1.2	42.3	4.7
$Ca_{12}Zr_{11}O_{28\_4}$	9	2.2	43.4	4.8	1.3	42.4	4.7
$Ca_{12}Zr_{10}O_{28\_1}$	10	0.0	30.9	3.1	0.0	29.8	3.0
$Ca_{12}Zr_{10}O_{28\_2}$	10	0.5	31.4	3.1	1.5	31.3	3.1
$Ca_{12}Zr_{10}O_{28\_3}$	10	1.9	32.8	3.3	1.2	31.0	3.1
$Ca_{12}Zr_{10}O_{28\_4}$	10	2.2	33.1	3.3	2.1	31.9	3.2
$Ca_{12}Zr_{12}O_{28\_1}$	8	0.0	51.9	6.5	0.0	51.5	6.4
$Ca_{12}Zr_{12}O_{28\_2}$	8	1.0	52.9	6.6	1.3	52.8	6.6
$Ca_{12}Zr_{12}O_{28\_3}$	8	2.9	54.8	6.8	2.7	54.2	6.8
$Ca_{11}Zr_{12}O_{26\_1}$	11	0.0	58.5	5.3	0.0	58.1	5.3
$Ca_{11}Zr_{12}O_{26\_2}$	11	1.9	60.4	5.5	2.1	60.1	5.5
$Ca_{11}Zr_{12}O_{26\_3}$	11	2.3	60.8	5.5	3.0	61.1	5.6

The following figures show side-view of the systems in Table S3.

The left column, (a)-labelled, shows the geometry before relaxation and includes the missing O/metal atoms represented by orange/yellow spheres. The right column, (b)-labelled, shows the geometry after relaxation, including lattice relaxation. Ca, Zr and O atoms are represented by blue, green and red spheres, respectively. The supercells are doubled in the *z* direction. The oxygen atoms appearing at the border of the image are due to the periodic boundary condition applied in the calculations.

- $Ca_{12}Zr_{11}O_{28\_1}$
  - GS

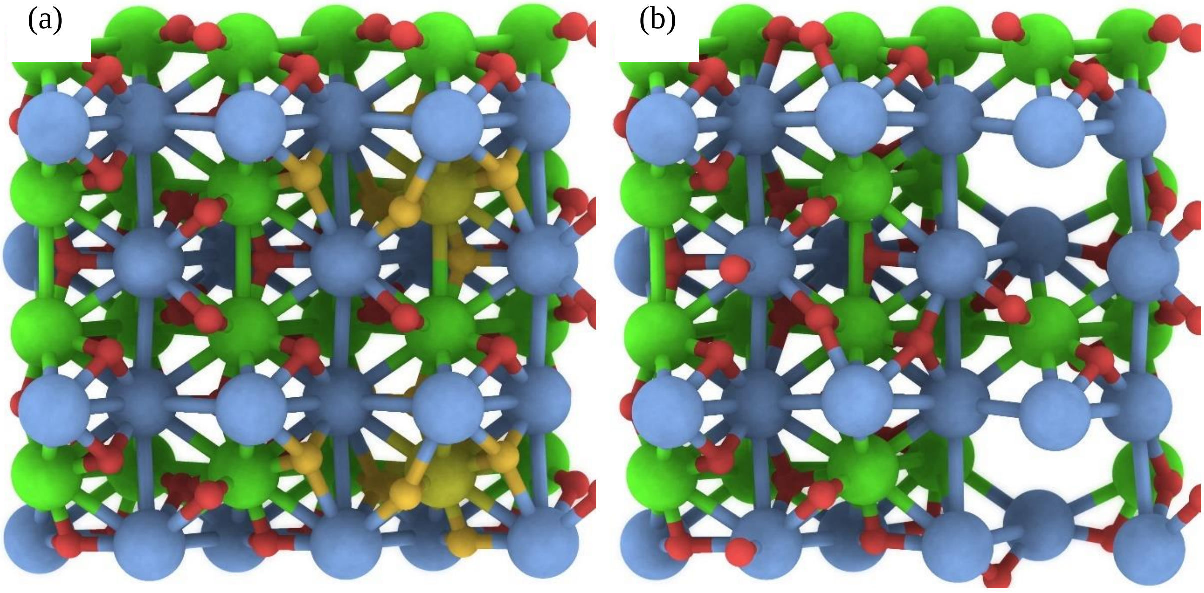

- $Ca_{12}Zr_{11}O_{28\_2}$
  - E_r = 1.3 eV

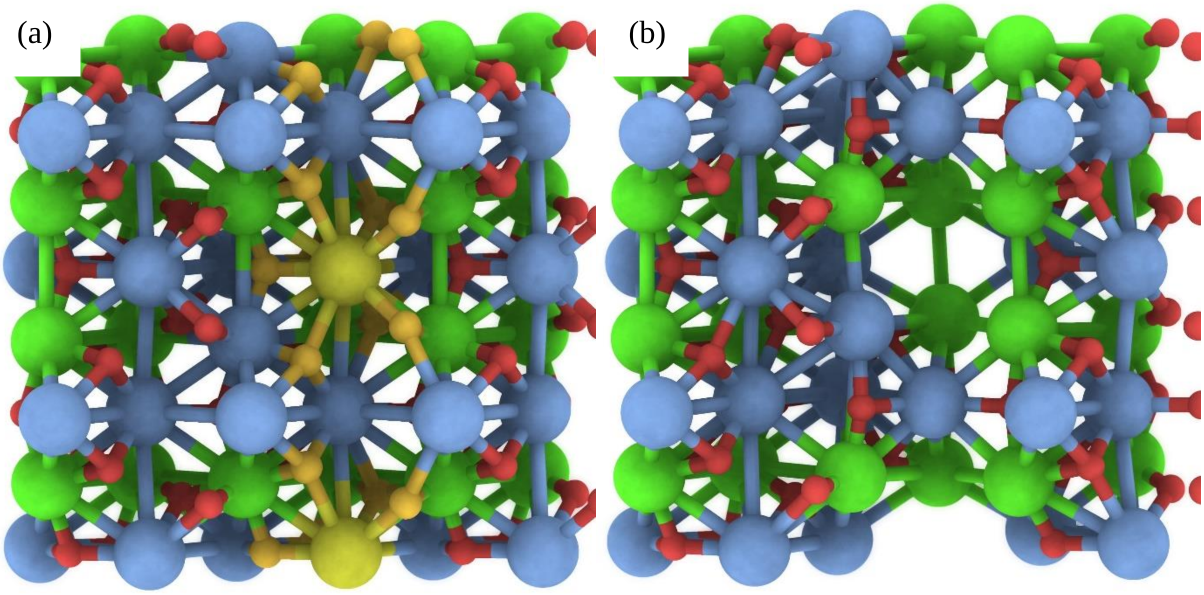

- $Ca_{12}Zr_{11}O_{28\_3}$
  - E_r = 1.8 eV

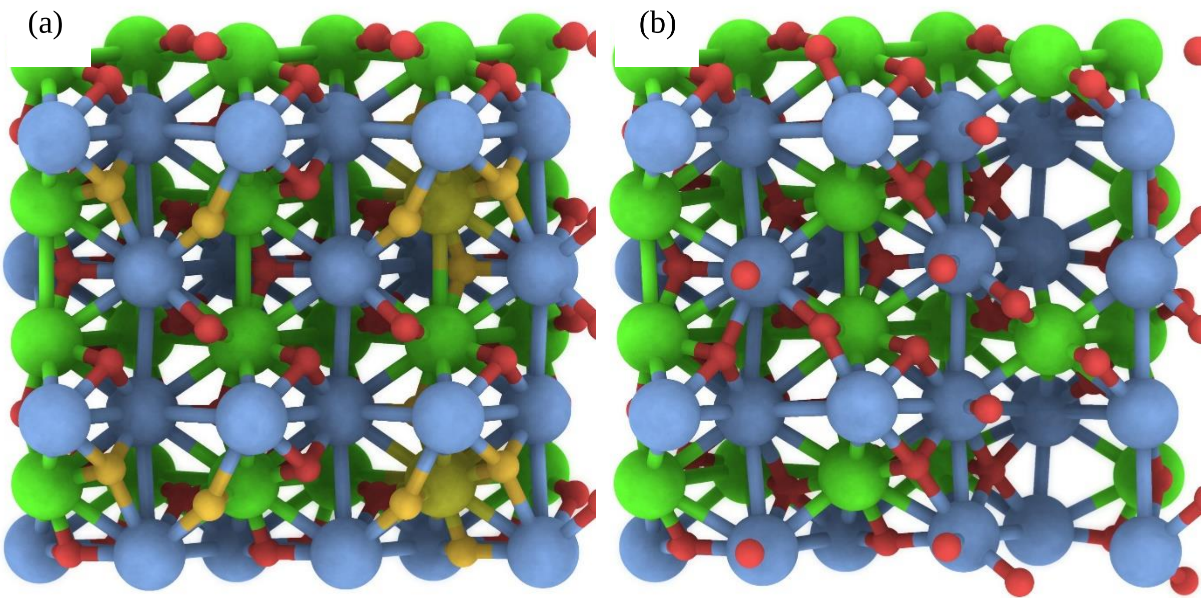

- $Ca_{12}Zr_{11}O_{28\_4}$
  - E_r = 2.2 eV

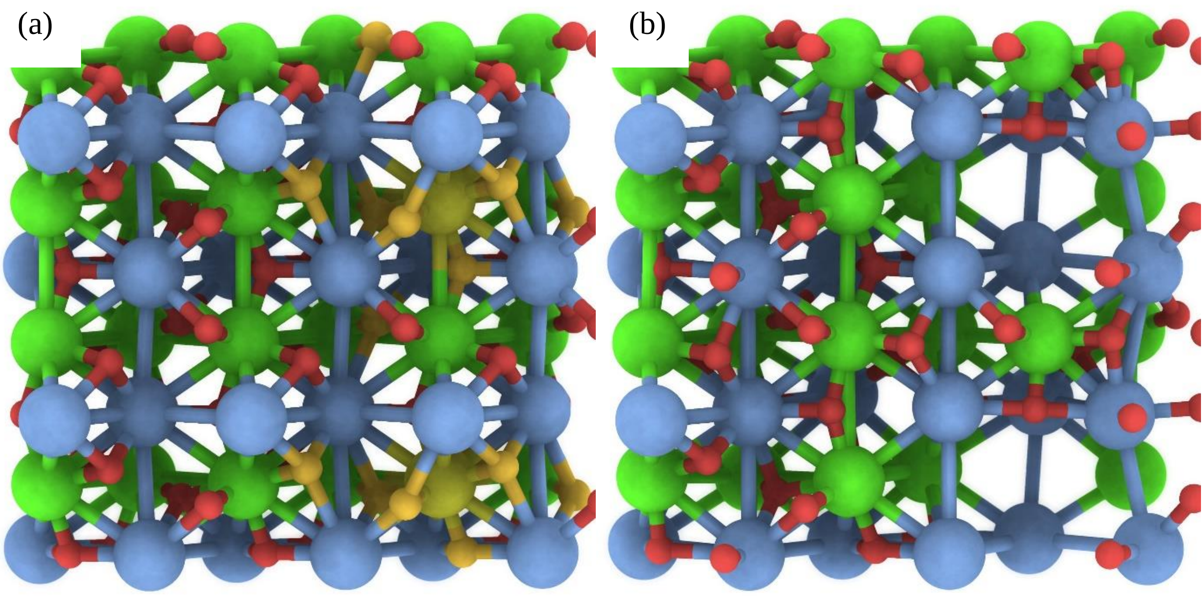

- $Ca_{12}Zr_{10}O_{28\_1}$
  - GS

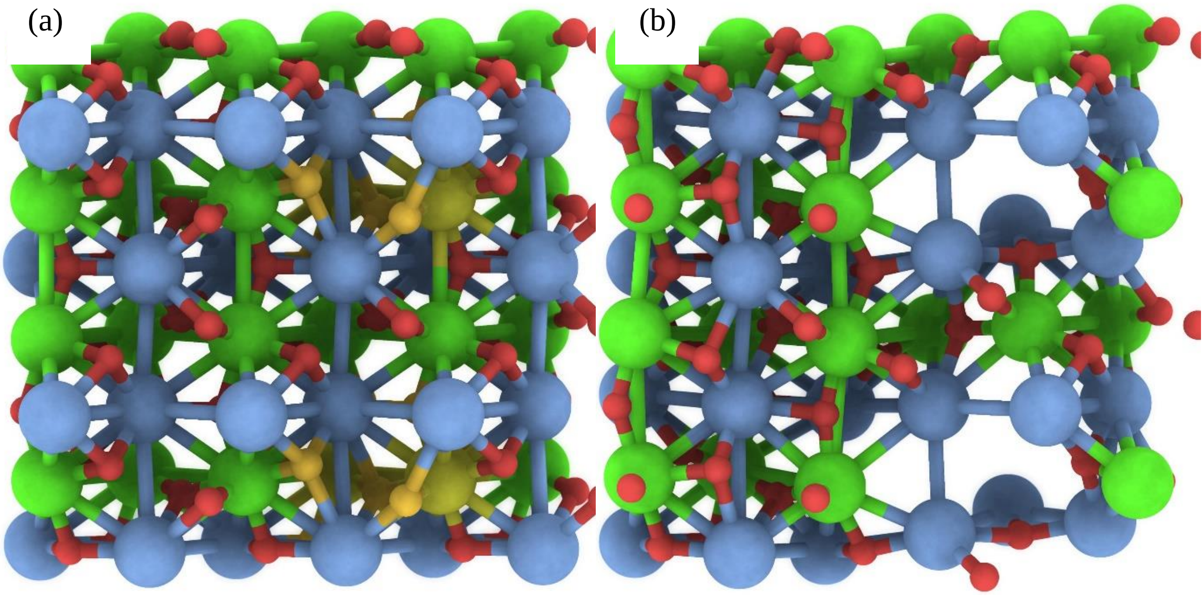

- $Ca_{12}Zr_{10}O_{28\_2}$
  - E_r = 0.5 eV

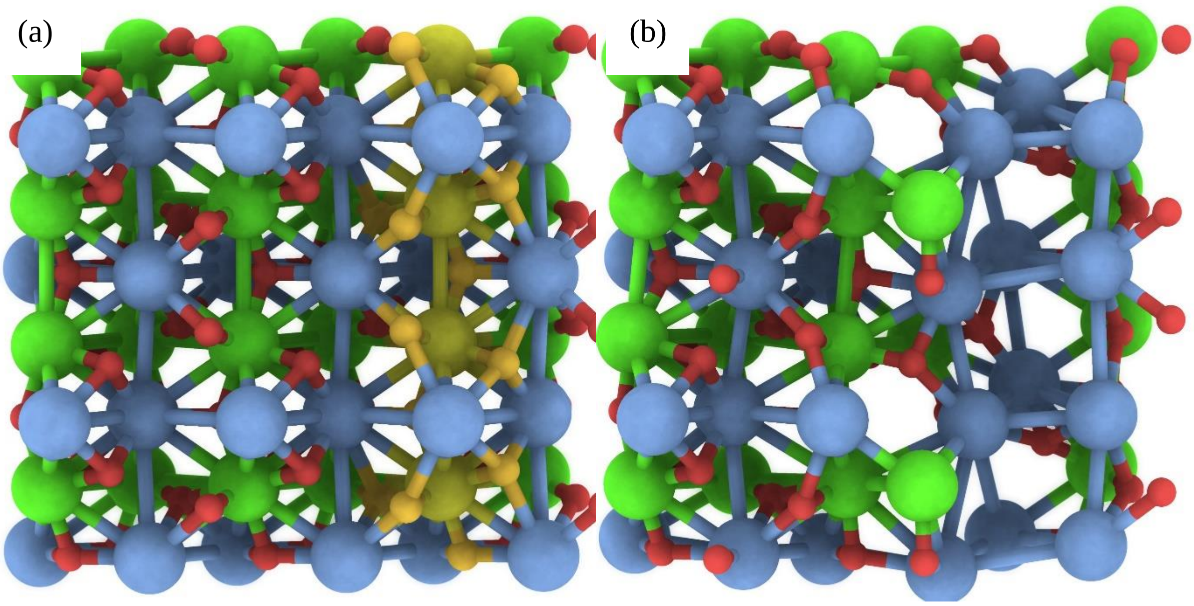

- $Ca_{12}Zr_{10}O_{28\_3}$
    - E_r = 1.9 eV

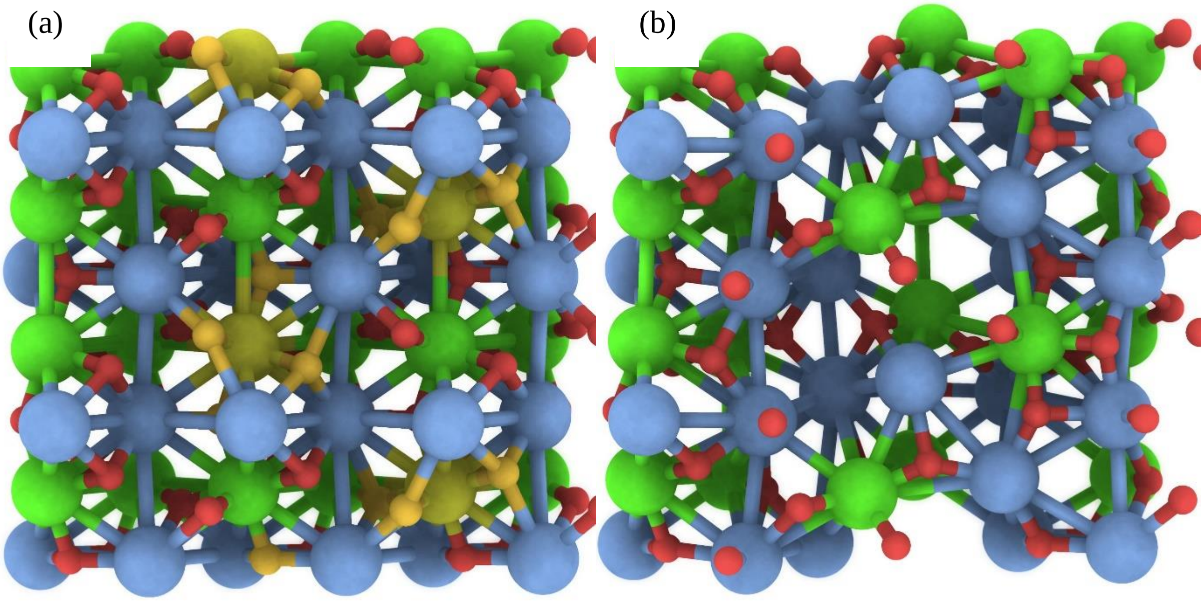

- $Ca_{12}Zr_{10}O_{28\_4}$
    - E_r = 2.2 eV

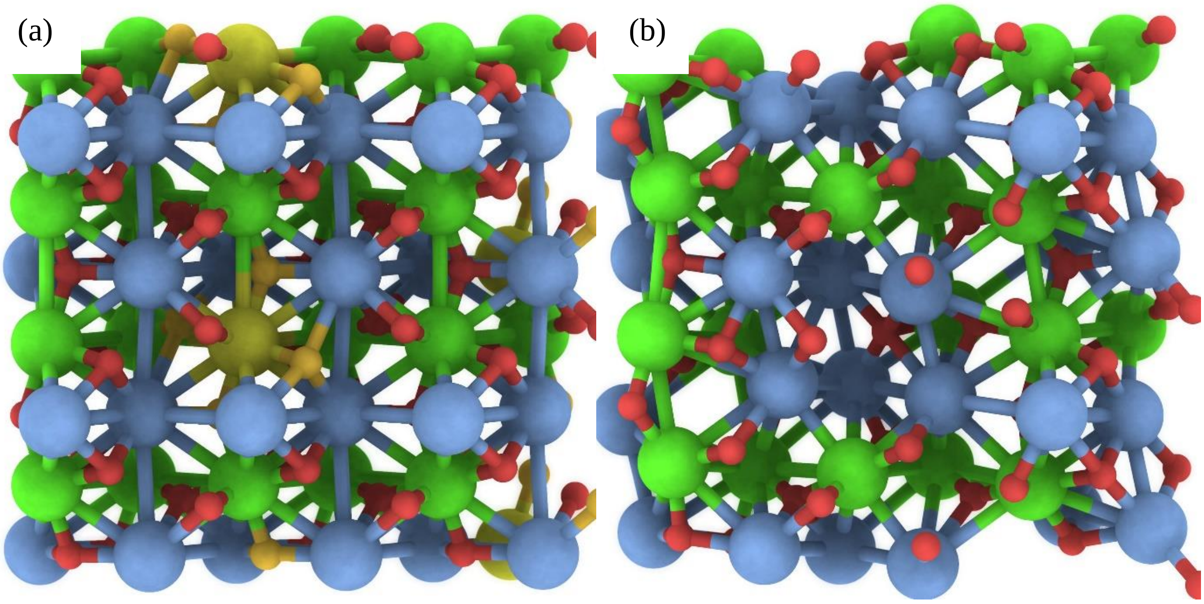

- $Ca_{12}Zr_{12}O_{28\_1}$
  - GS

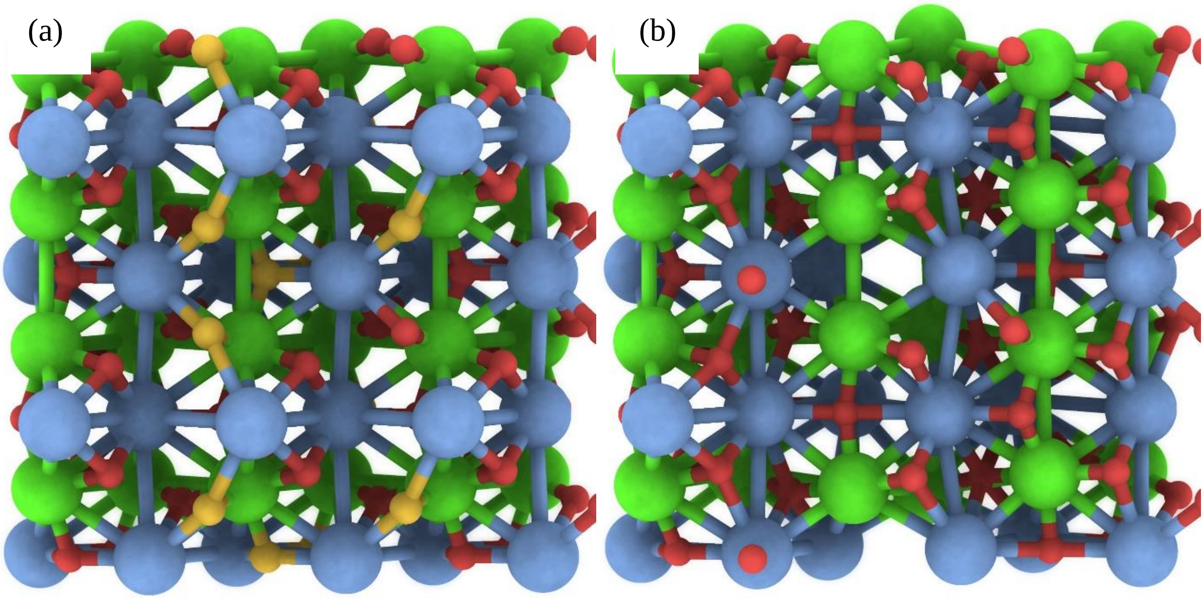

- $Ca_{12}Zr_{12}O_{28\_2}$
  - $E_r = 1.0$ eV

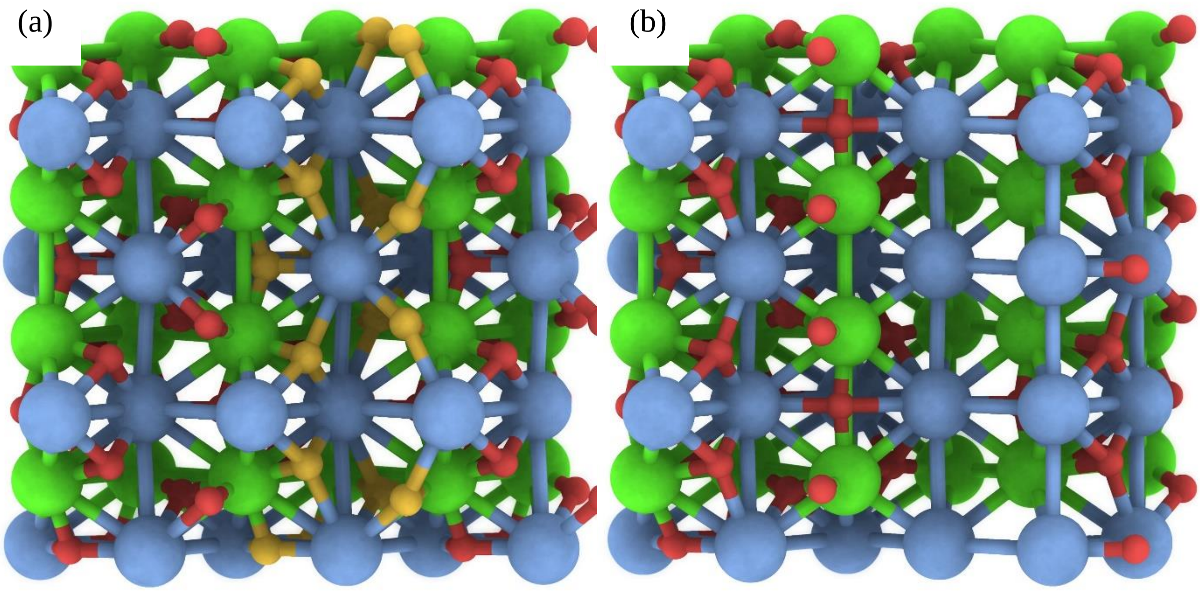

- $Ca_{12}Zr_{12}O_{28\_3}$
  - E_r = 2.9 eV

(a)

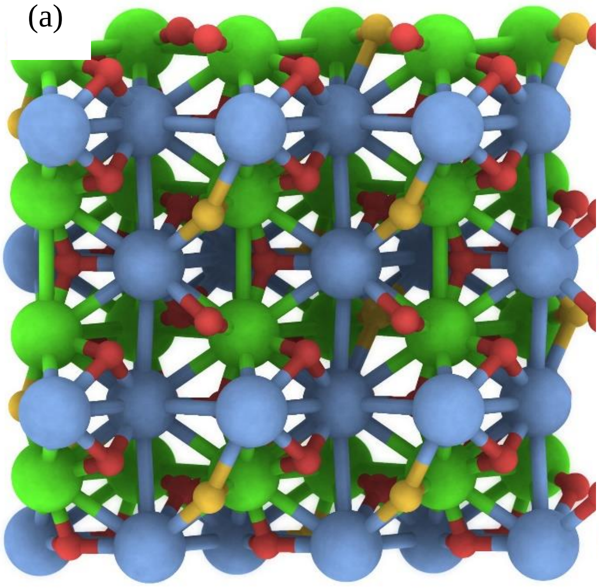

(b)

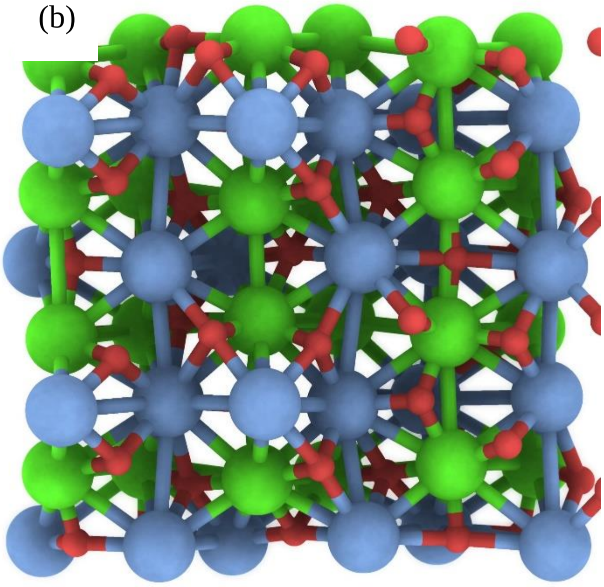

- $Ca_{11}Zr_{12}O_{26\_1}$
  - GS

(a)

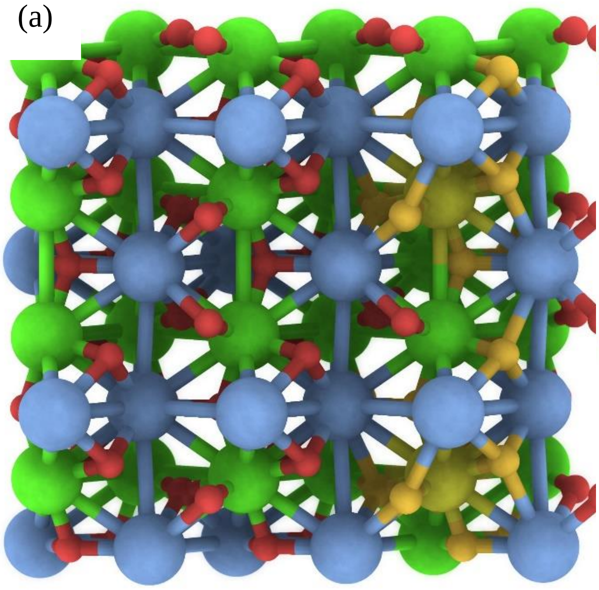

(b)

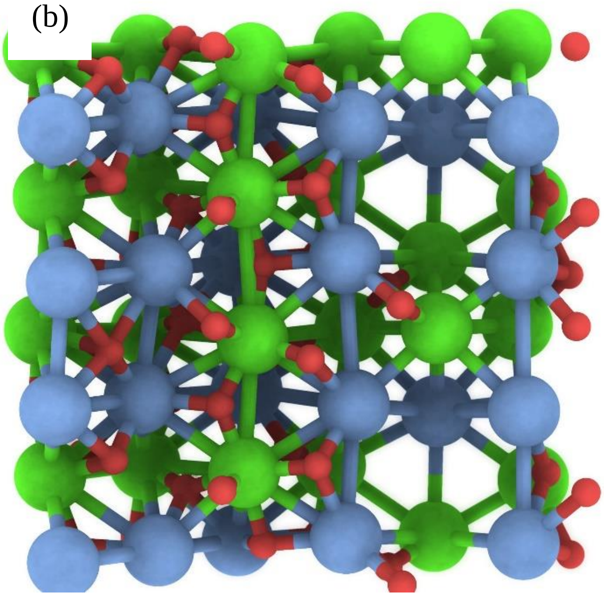

- $Ca_{11}Zr_{12}O_{26\_2}$
    - E_r = 1.9 eV

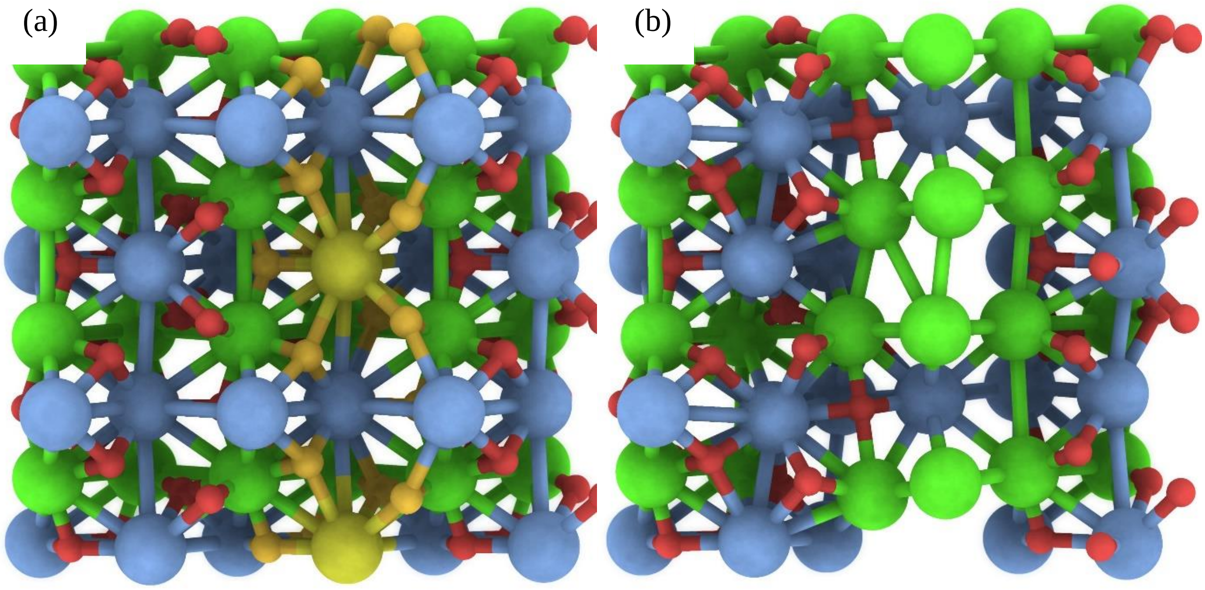

- $Ca_{11}Zr_{12}O_{26\_3}$
    - E_r = 2.3 eV

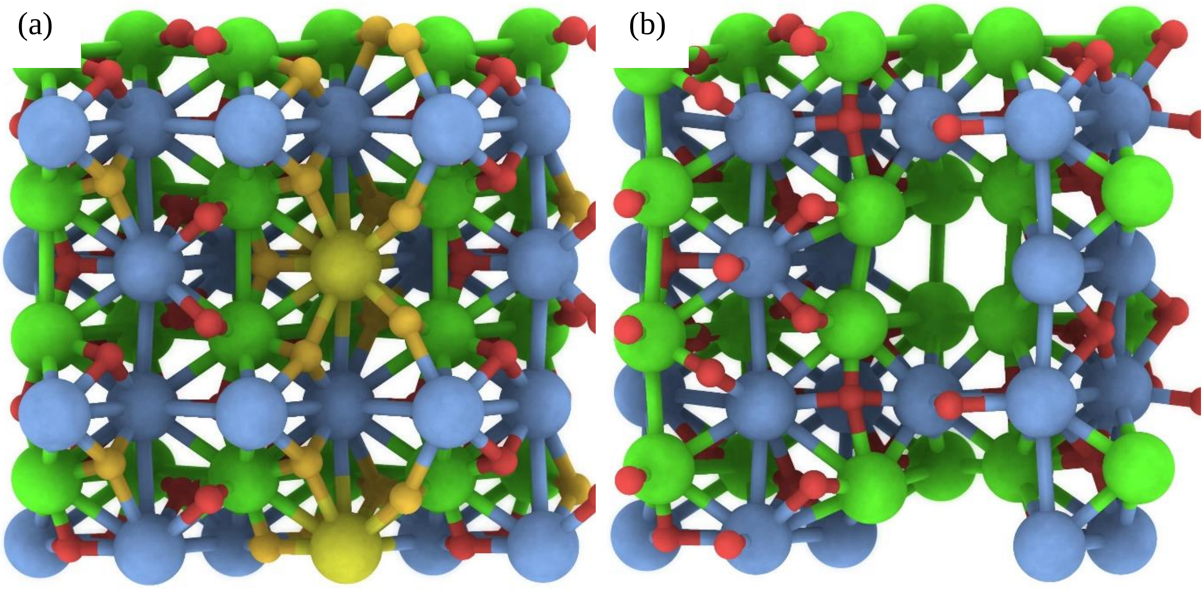

Table S4. Dependence of cleavage energy ($E_{s,c}$) and surface energy (E_s), both in J/m^2, on the number of layers (slab thickness). At least 4-layer slab is needed to model the (111)

Number of layers	2	3	4	5	6	7
$E_{s,c,001}$	0.87	0.87	0.87	0.87	0.87	0.87
$E_{s,001}$ (CaO termination)	0.75	0.74	0.74	0.74	0.73	0.73
$E_{s,001}$ (ZrO_2 termination)	0.74	0.72	0.72	0.71	0.71	0.71
$E_{s,c,110}$	1.15	1.16	1.16	1.16	1.16	1.15
$E_{s,110}$	0.65	0.69	0.67	0.67	0.67	0.67
$E_{s,c,111}$	1.28	1.30	1.30	1.33	1.34	1.31
$E_{s,111}$ (CaO termination)	1.02	0.84	0.90	0.94	-	-
$E_{s,111}$ (ZrO_2 termination)	0.62	0.75	0.98	0.99	-	-

Table S5. Multiple defects formed at the (001) surface with the initial stoichiometry $Ca_{32}Zr_{32}O_{96}$. All energies are in eV

System	N	E_r	E_{df}	E_{df}/N
$Ca_{32}Zr_{32}O_{75\_1}$	21	0.0	158.9	7.6
$Ca_{32}Zr_{32}O_{75\_2}$	21	1.5	160.5	7.6
$Ca_{32}Zr_{32}O_{75\_3}$	21	12.5	171.4	8.2
$Ca_{32}Zr_{32}O_{75\_4}$	21	16.9	175.8	8.4
$Ca_{29}Zr_{32}O_{69\_1}$	30	0.0	224.4	7.5
$Ca_{29}Zr_{32}O_{69\_2}$	30	2.0	226.4	7.5
$Ca_{29}Zr_{32}O_{69\_3}$	30	6.4	230.8	7.7
$Ca_{29}Zr_{32}O_{69\_4}$	30	16.9	241.3	8.0

The following figures show side-view of the systems in Table S5. The supercells are doubled the *x* and *y* directions.

- $Ca_{32}Zr_{32}O_{75\_1}$
  - GS

(a)

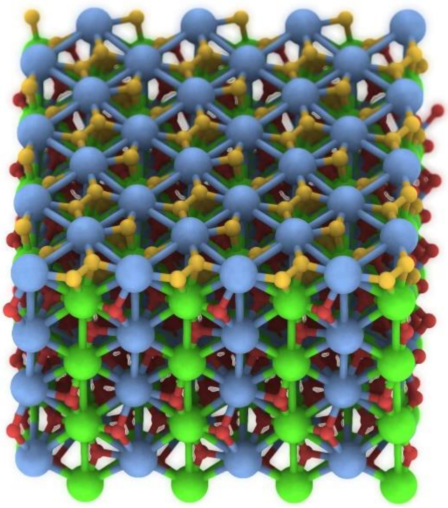

(b)

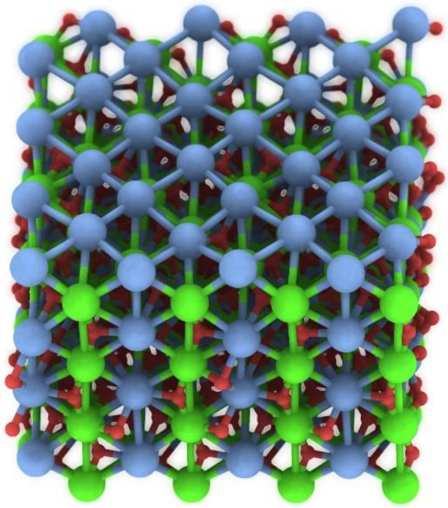

- $Ca_{32}Zr_{32}O_{75\_2}$
  - E_r = 1.5 eV

(a)

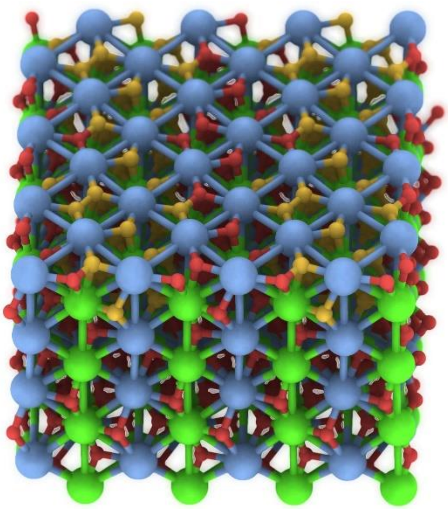

(b)

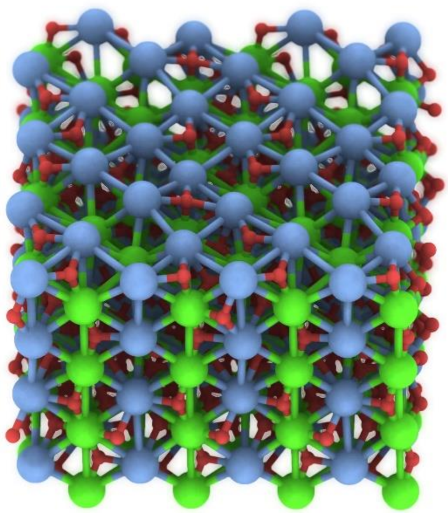

- $Ca_{32}Zr_{32}O_{75\_3}$
  - E_r = 12.5 eV

(a)

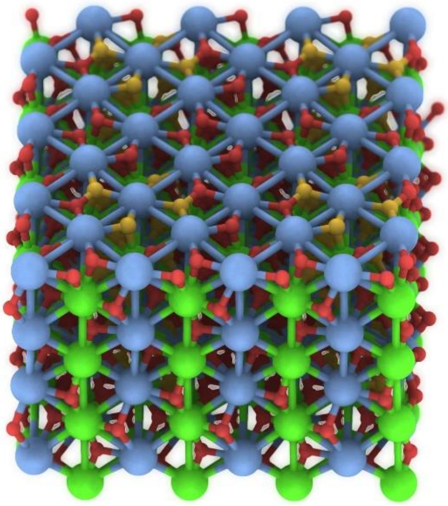

(b)

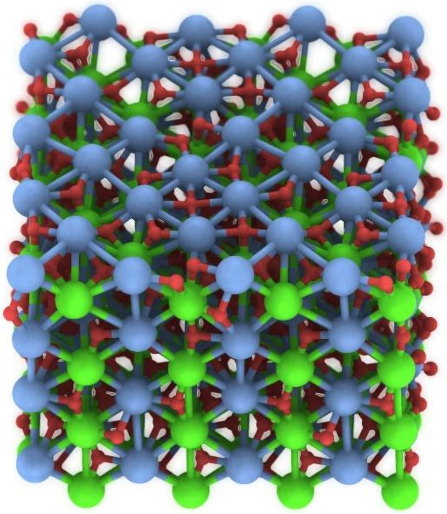

- $Ca_{32}Zr_{32}O_{75\_4}$
  - E_r = 16.9 eV

(a)

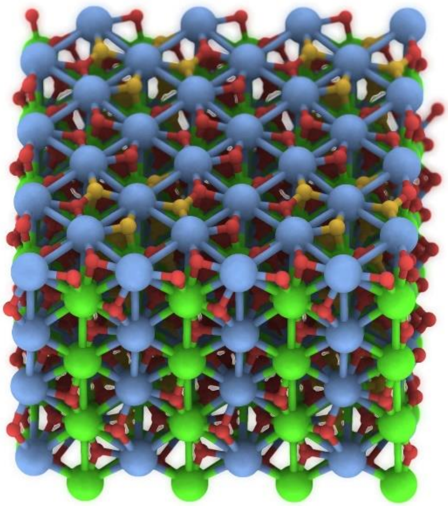

(b)

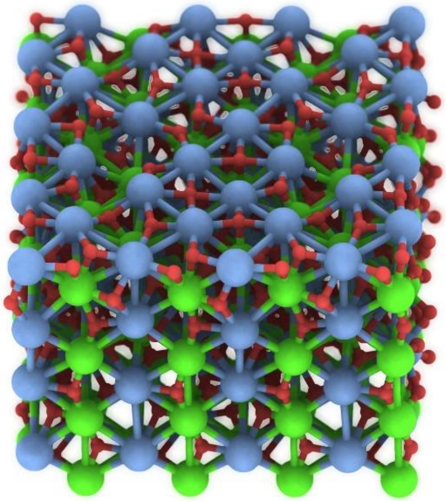

- $Ca_{29}Zr_{32}O_{69\_1}$
  - GS

(a)

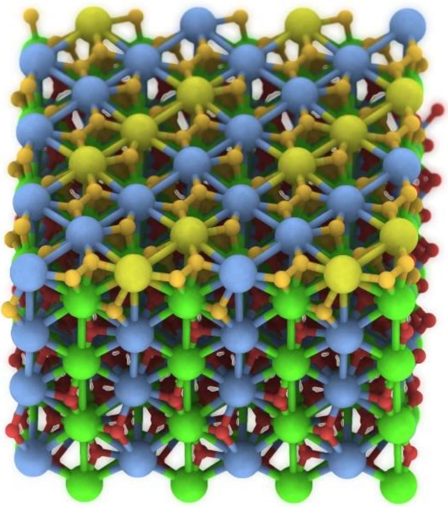

(b)

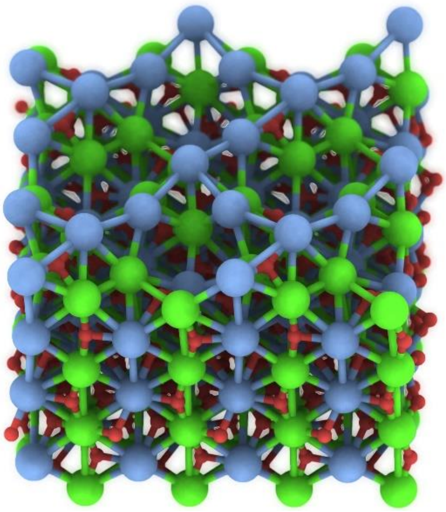

- $Ca_{29}Zr_{32}O_{69\_2}$
  - E_r = 2.0 eV

(a)

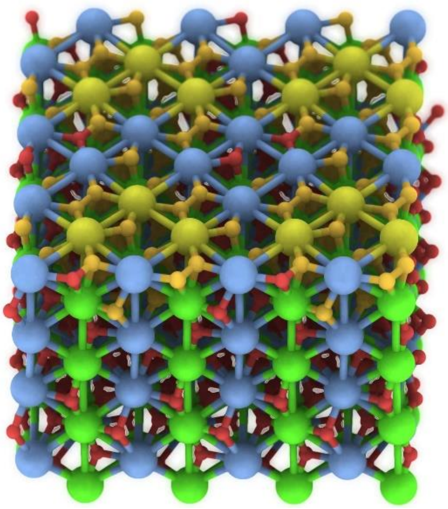

(b)

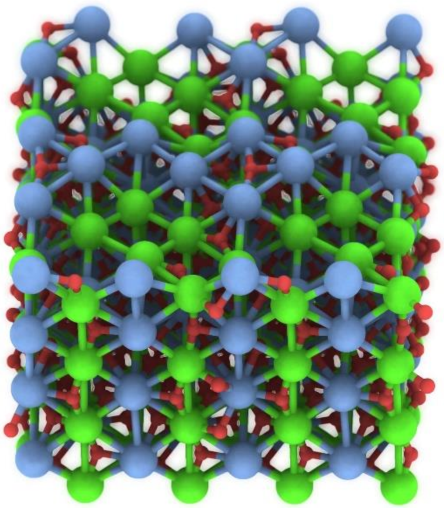

- $Ca_{29}Zr_{32}O_{69}$_3
    - E_r = 6.4 eV

(a)

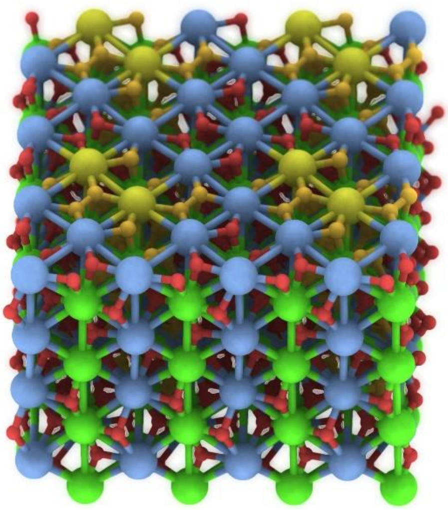

(b)

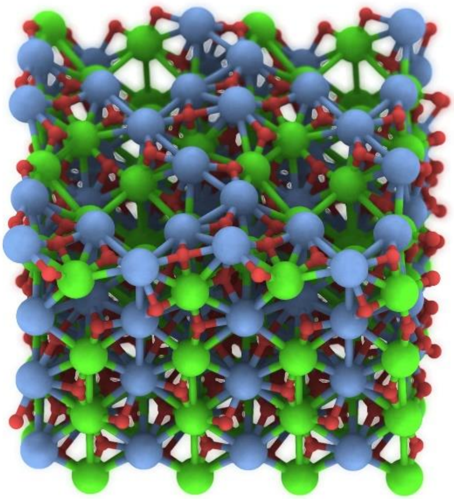

- $Ca_{29}Zr_{32}O_{69}$_4
    - E_r = 16.9 eV

(a)

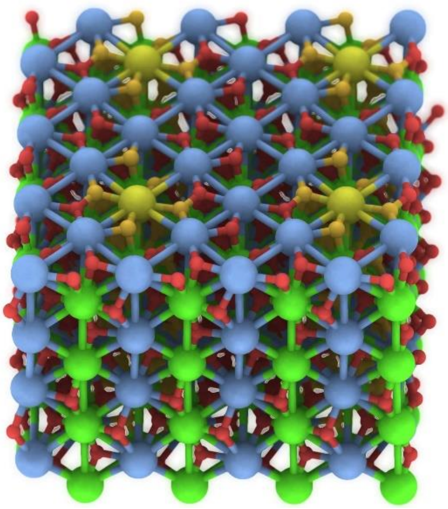

(b)

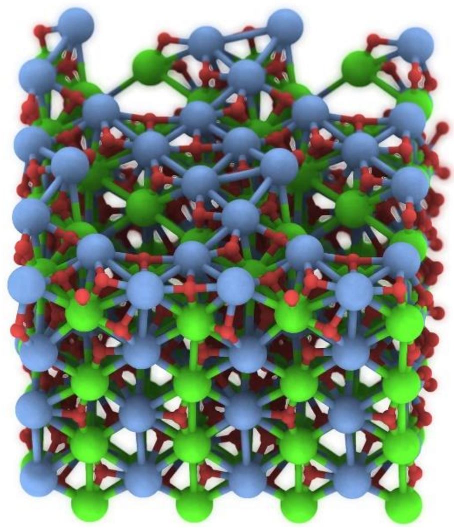

Section S4: DFT results – O and Ca migrations in single-defect systems

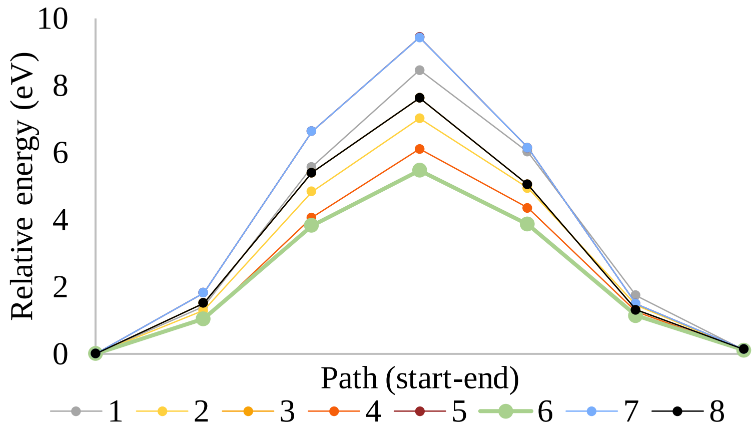

Figure S4. Energy profile for O migration in an orthorhombic supercell with a single O vacancy. O moves from the occupied O position to the vacant O position. The relative energy is calculated with respect to the initial geometry. The geometry of the most and least energetically favourable O migration path is shown in Fig. S5. The geometries of all paths labelled with the number shown in the legend are displayed in the following images

Figure S5. Bulk crystal structure of $CaZrO_3$ (a). The most (b) and least (c) energetically favourable path for O migration enclosed by the black circle (path 6 and path 7 in Fig. S4,

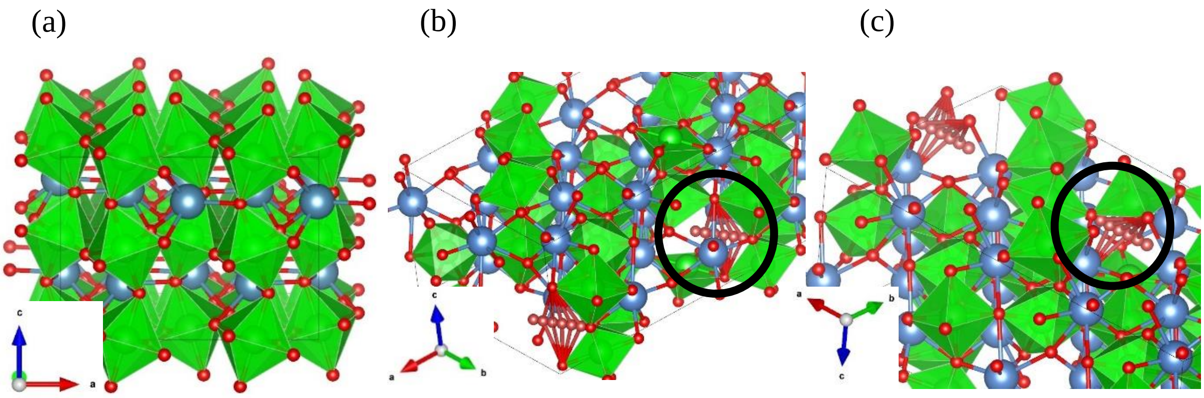

respectively, from the apex of the ZrO6 octahedron to the apex of the adjacent ZrO6 octahedron and along the edge of the ZrO6 octahedron

The images below show the migration of an O atom along energy paths in Fig. S4. The bright red atoms enclosed by the black circle represent the migrating O atom. The left (a) and right (b) columns show the same path viewed from a wider and closer perspective, and from different angles, respectively.

○ 1)

(a)

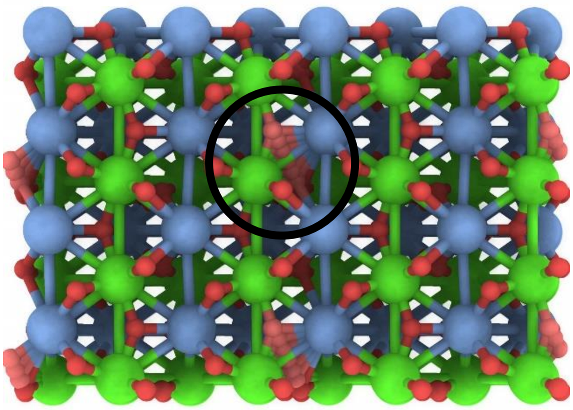

(b)

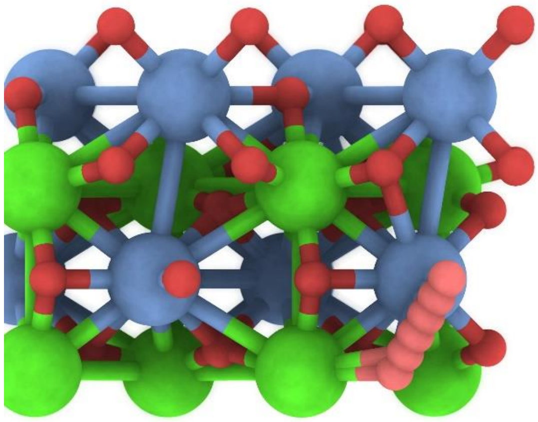

○ 2)

(a)

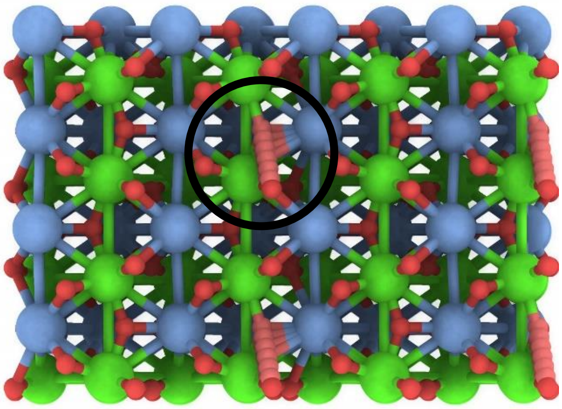

(b)

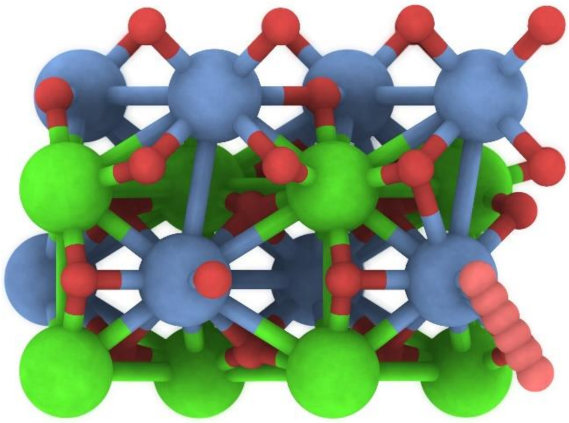

○ 3)

(a)

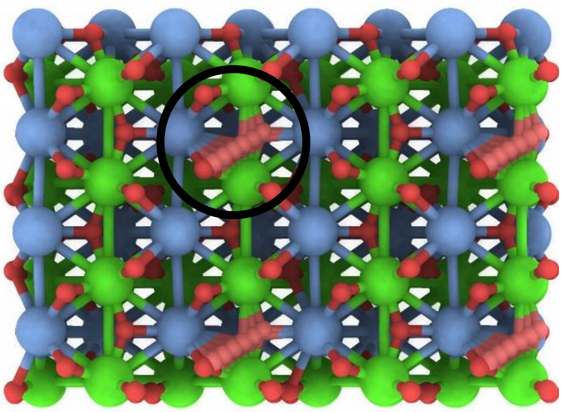

(b)

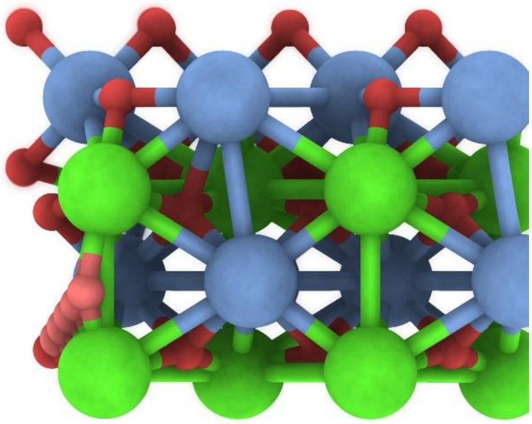

○ 4)

(a)

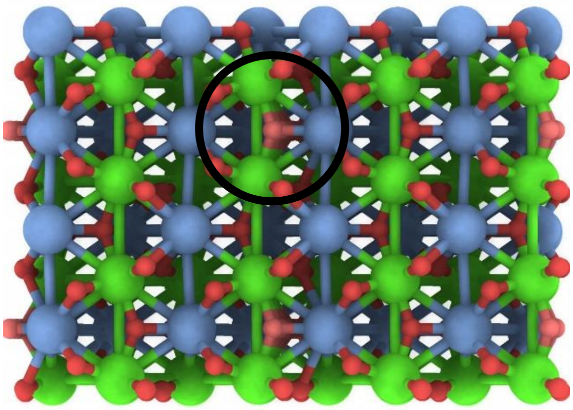

(b)

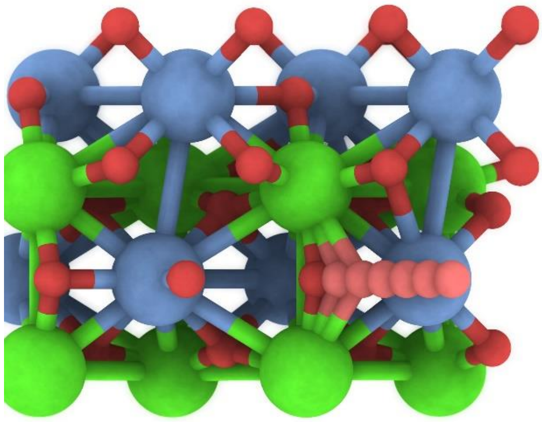

○ 5)

(a)

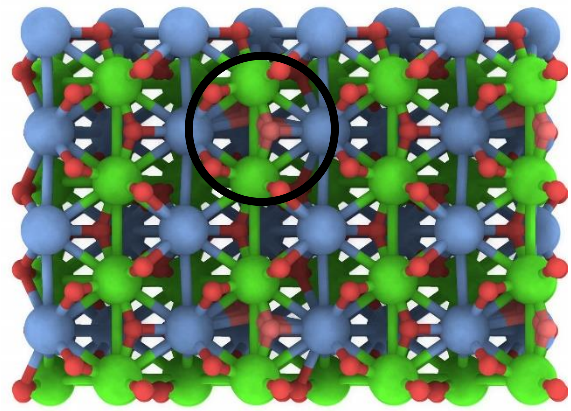

(b)

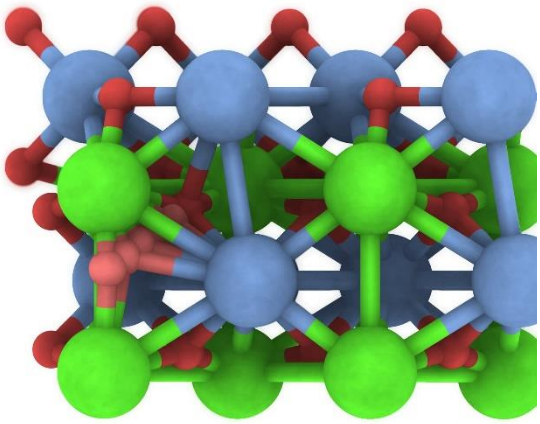

○ 6)

(a)

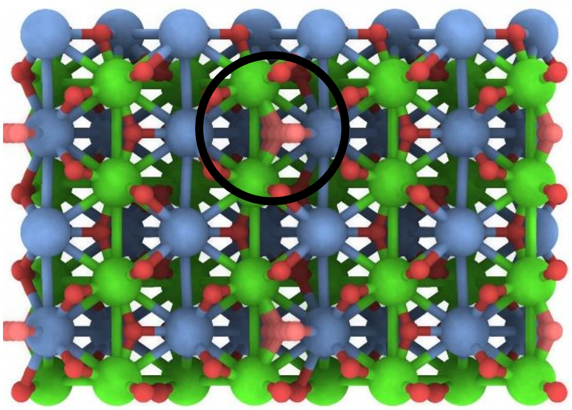

(b)

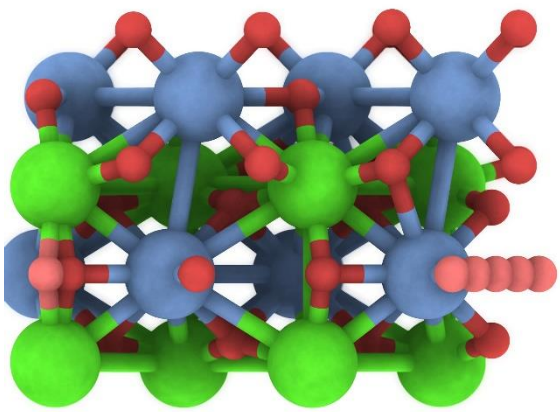

○ 7)

(a)

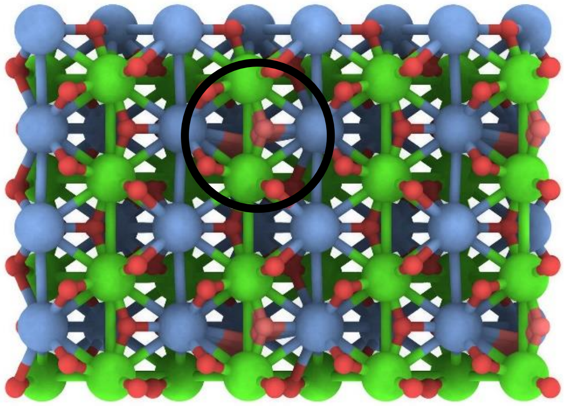

(b)

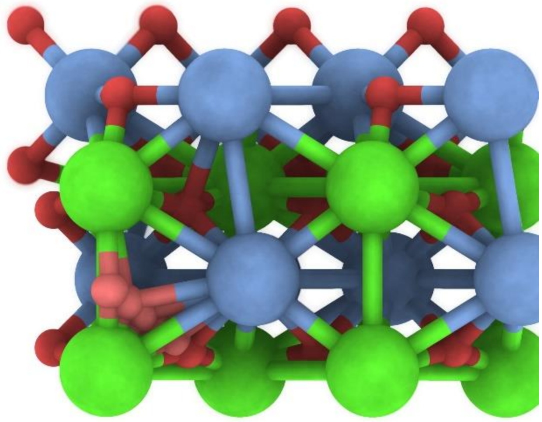

○ 8)

(a)

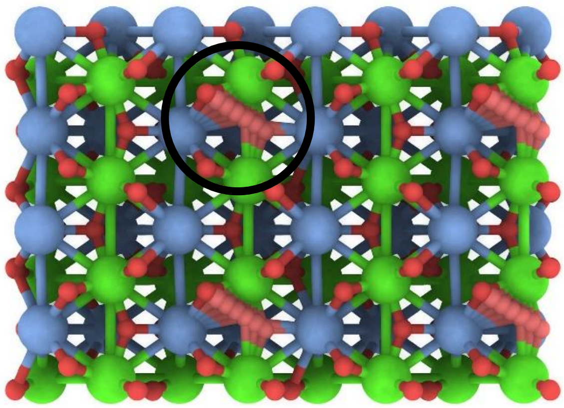

(b)

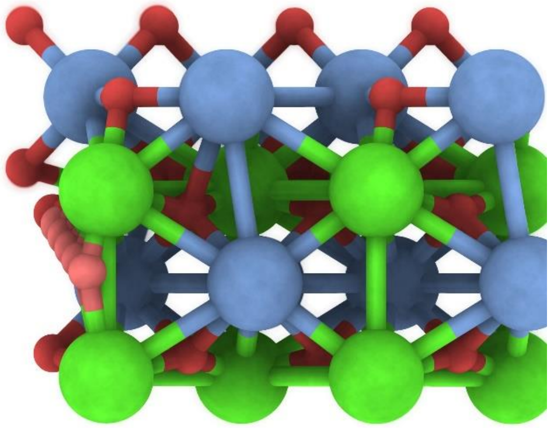

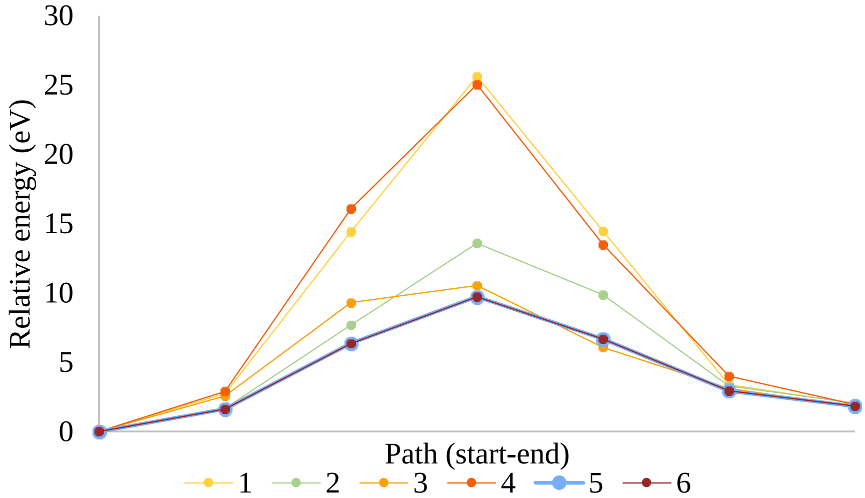

Figure S6. Energy profile for Ca migration in an orthorhombic supercell of $CaZrO_3$ with a Ca defect. Ca moves from the occupied Ca position to the vacant Ca position. The relative energy is calculated with respect to the initial supercell. The geometry of the most (5) and least (1) energetically favourable Ca migration path is shown in Fig. S7. The geometries of all paths labelled with the number shown in the legend are displayed in the following images

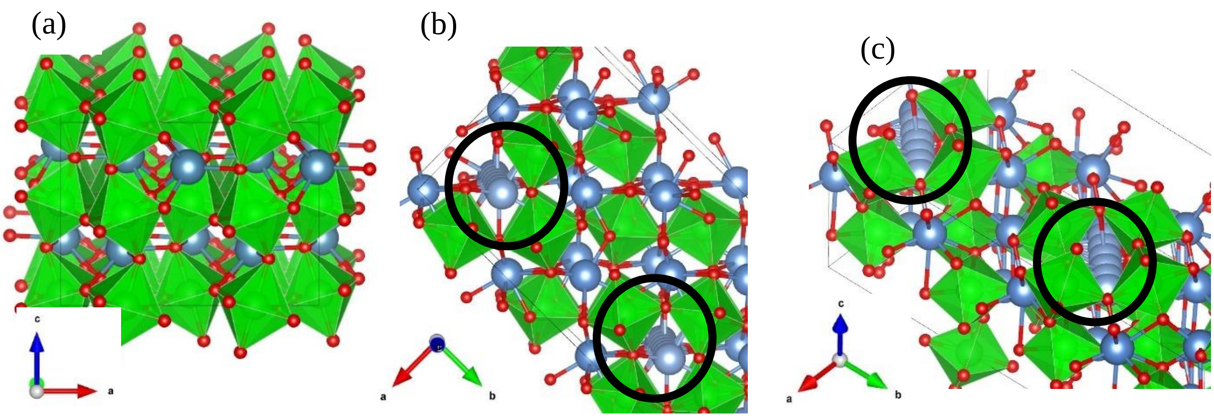

Figure S7. Bulk crystal structure of $CaZrO_3$ (a). The most (b) and least (c) energetically favourable path for Ca migration enclosed by the black circles (path 5 and path 1 in Fig. S6, respectively, both through the space between ZrO_6 octahedra)

The images below show the migration of a Ca atom along energy paths shown in Fig. S6. The bright blue atoms enclosed by the black circle represent the migrating Ca atom. The left (a) and right (b) columns show the same path viewed from the side (wider) and top (closer) view, respectively.

○ 1)

(a)

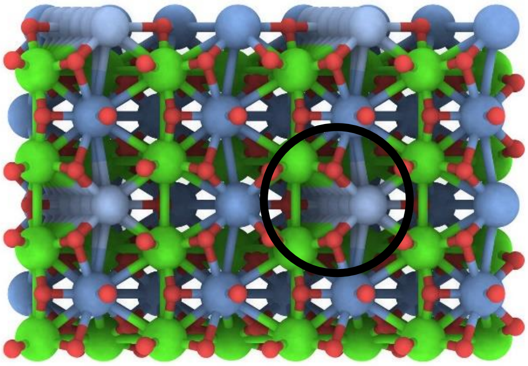

(b)

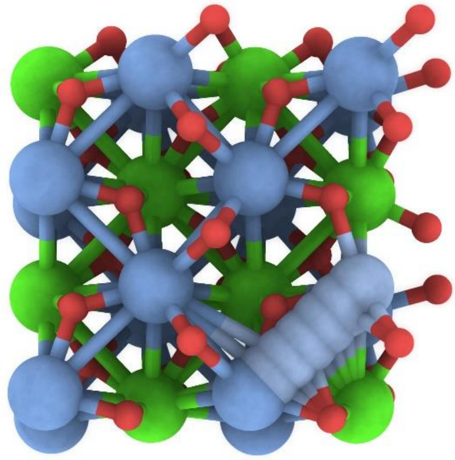

○ 2)

(a)

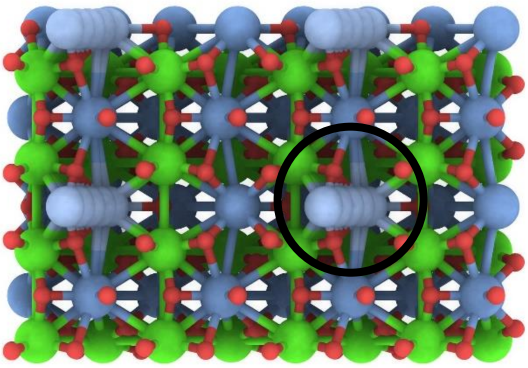

(b)

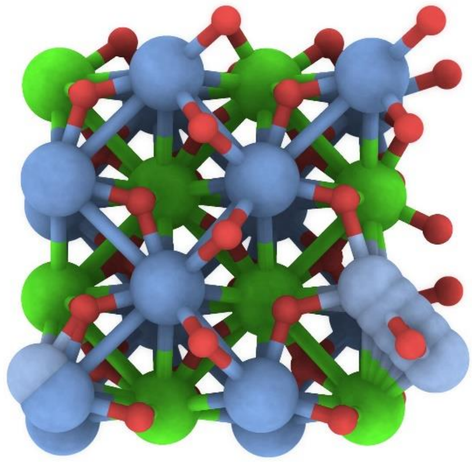

○ 3)

(a)

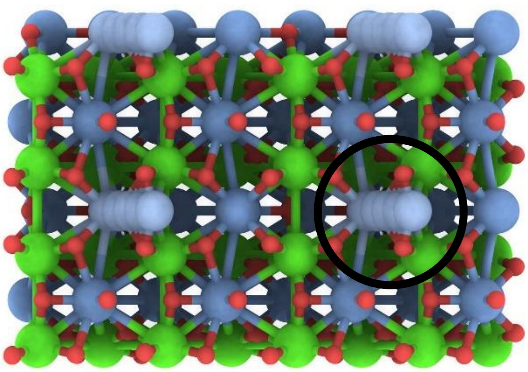

(b)

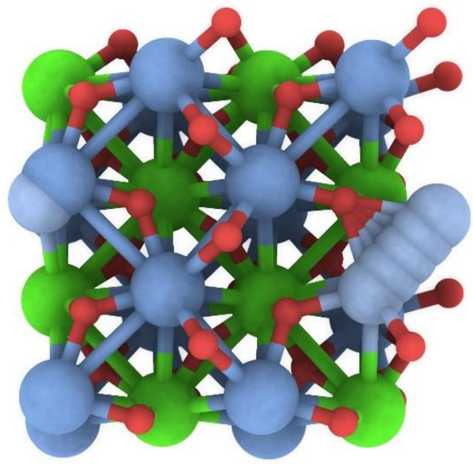

○ 4)

(a)

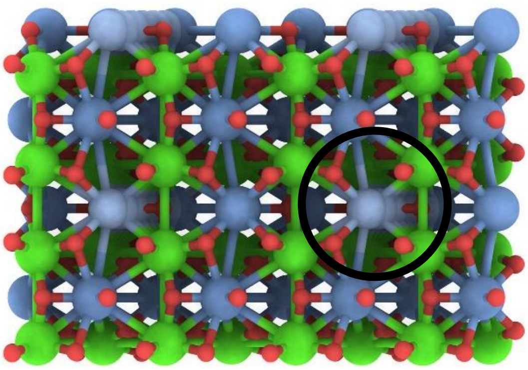

(b)

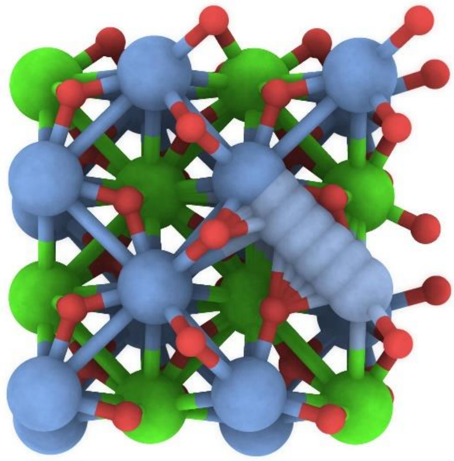

○ 5)

(a)

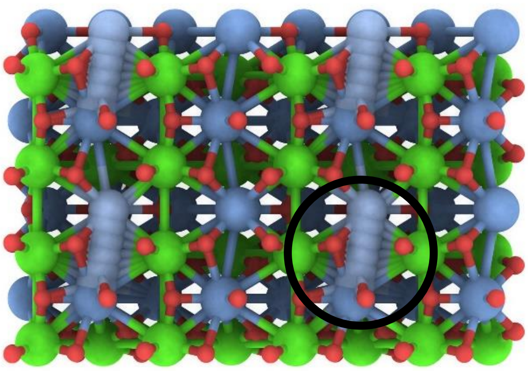

(b)

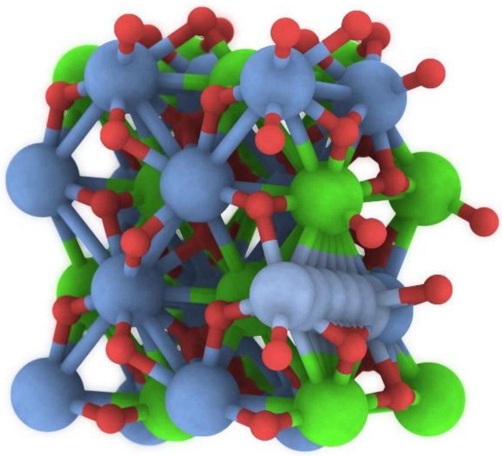

○ 6)

(a)

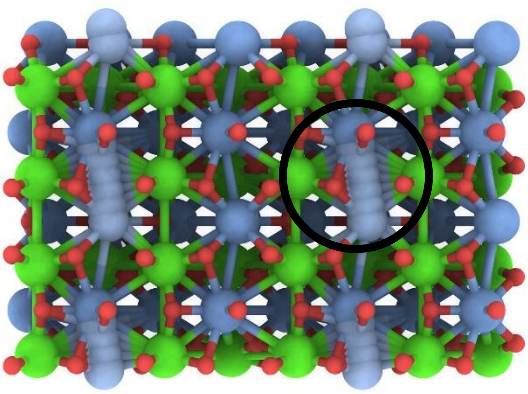

(b)

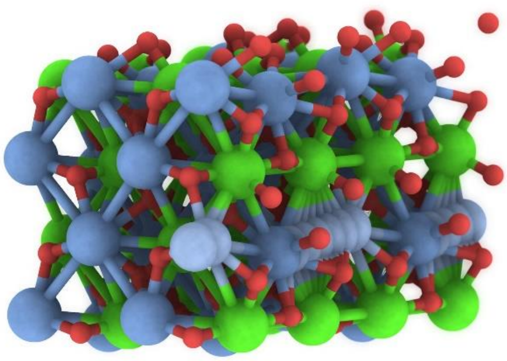

Section S5: DFT results – O, Ca, and Zr migrations in multiple-defect systems

Table S7. Energy barriers (in eV) for O migration. The geometries of all paths are shown under the energy profiles below

System	Label 01	02	03	04	05
$Ca_{12}Zr_{11}O_{28\_1}$	2.6	**1.6**	2.3		
$Ca_{12}Zr_{10}O_{28\_1}$	4.8	**1.9**	3.4		
$Ca_{12}Zr_{12}O_{28\_1}$	4.9	**3.9**			
$Ca_{11}Zr_{12}O_{26\_1}$	4.7	5.5	3.1	**1.9**	4.9

Table S8. Energy barriers (in eV) for Ca migration. The geometries of all paths are shown under the energy profiles below

System	Label 03	04	05	06	07	08	09	10	11	12	13	14
$Ca_{12}Zr_{11}O_{28\_1}$		9.2	14.5	10.1	**5.3**	15.3	7.4					
$Ca_{12}Zr_{10}O_{28\_1}$		18.1	11.5	10.8	8.6	9.7	2.4	**1.2**				
$Ca_{12}Zr_{12}O_{28\_1}$	12.2	8.1	3.9	**2.0**	16.5	10.6						
$Ca_{11}Zr_{12}O_{26\_1}$				18.3	19.0	12.8	14.6	18.3	**5.6**	8.3	9.9	14.9

Two migration paths for Zr were also considered. The barriers are 5.4 eV and 3.5 eV, respectively. The geometries of both paths ($Ca_{12}Zr_{12}O_{28\_09}$ and $Ca_{11}Zr_{12}O_{26\_1\_15}$) are shown under the energy profiles below.

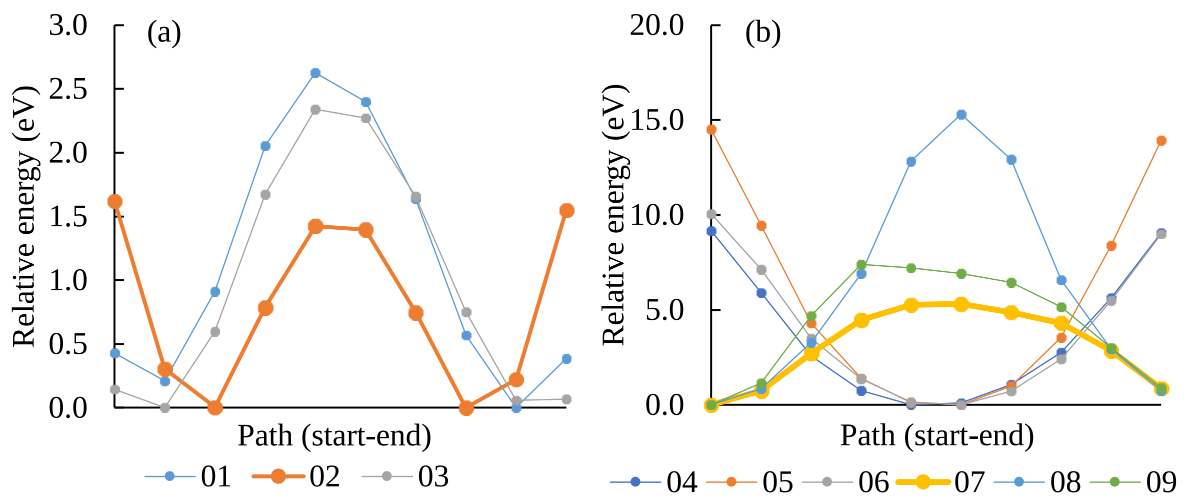

Figure S8. Energy profiles for O (a) and Ca (b) migrations in $Ca_{12}Zr_{11}O_{28\_1}$.

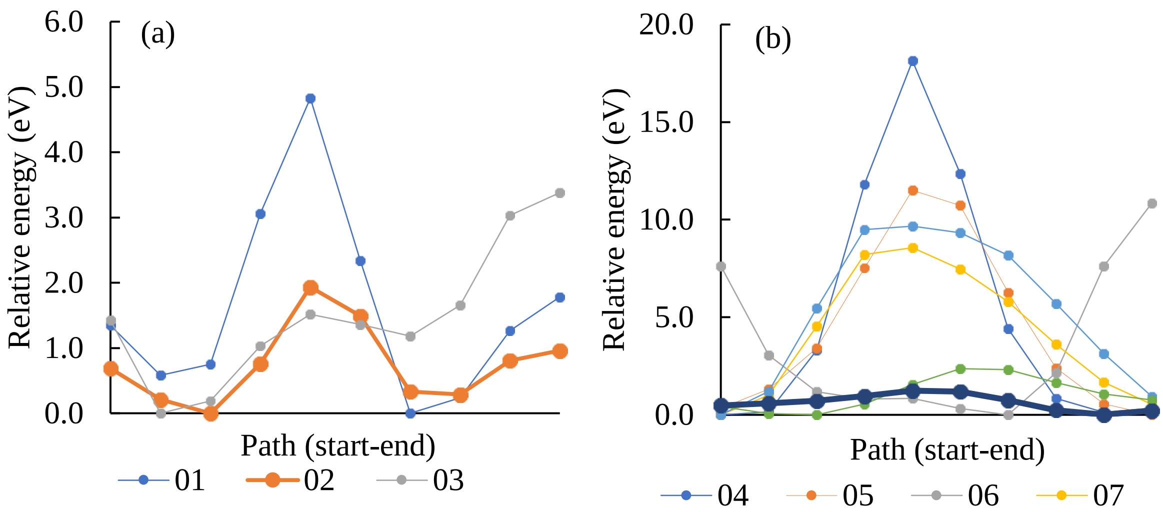

Figure S9. Energy profiles for O (a) and Ca (b) migrations in $Ca_{12}Zr_{10}O_{28\_1}$.

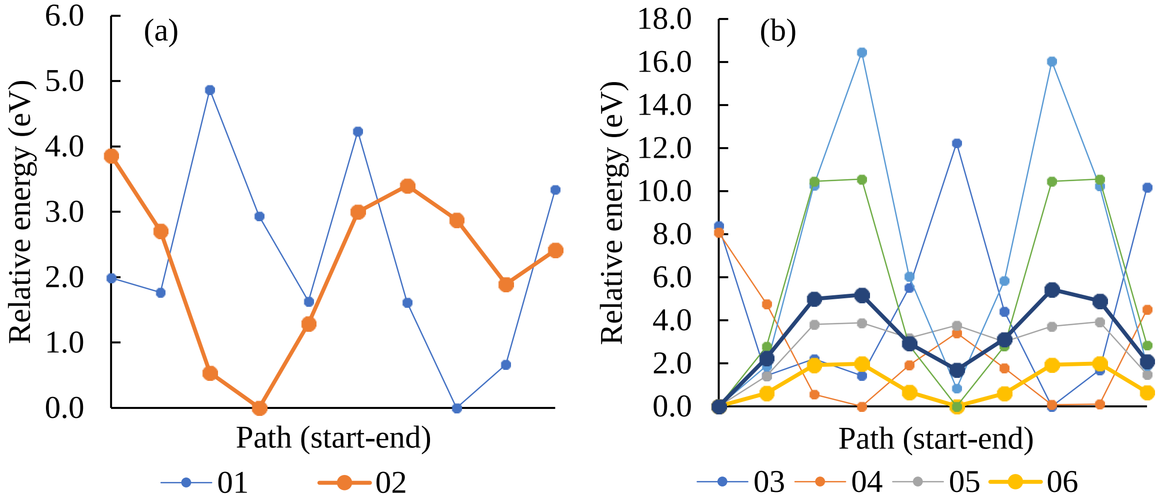

Figure S10. Energy profiles for O (a) and Ca and Zr (b) migrations in $Ca_{12}Zr_{12}O_{28\_1}$.

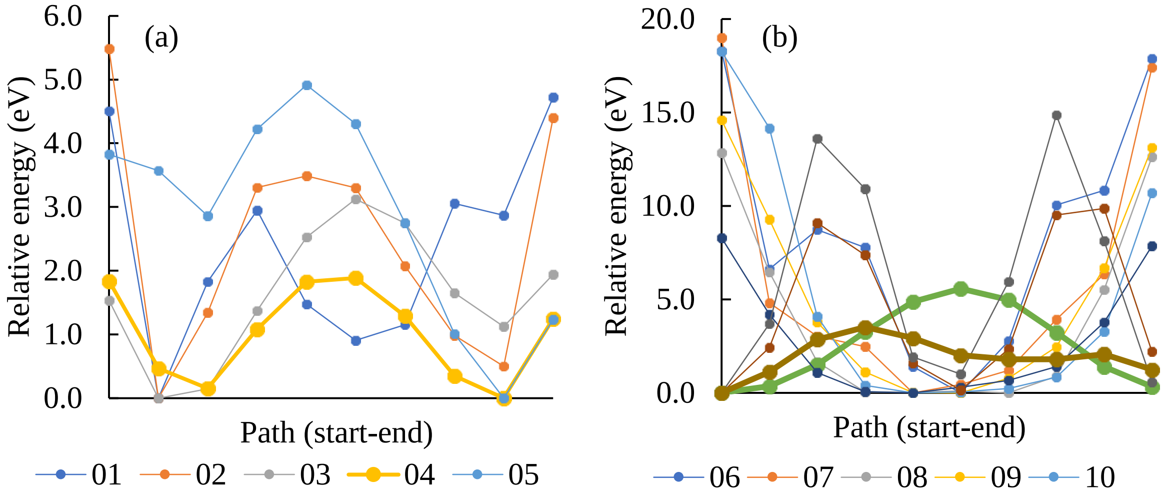

Figure S11. Energy profiles for O (a) and Ca and Zr (b) migrations in $Ca_{11}Zr_{12}O_{26\_1}$.

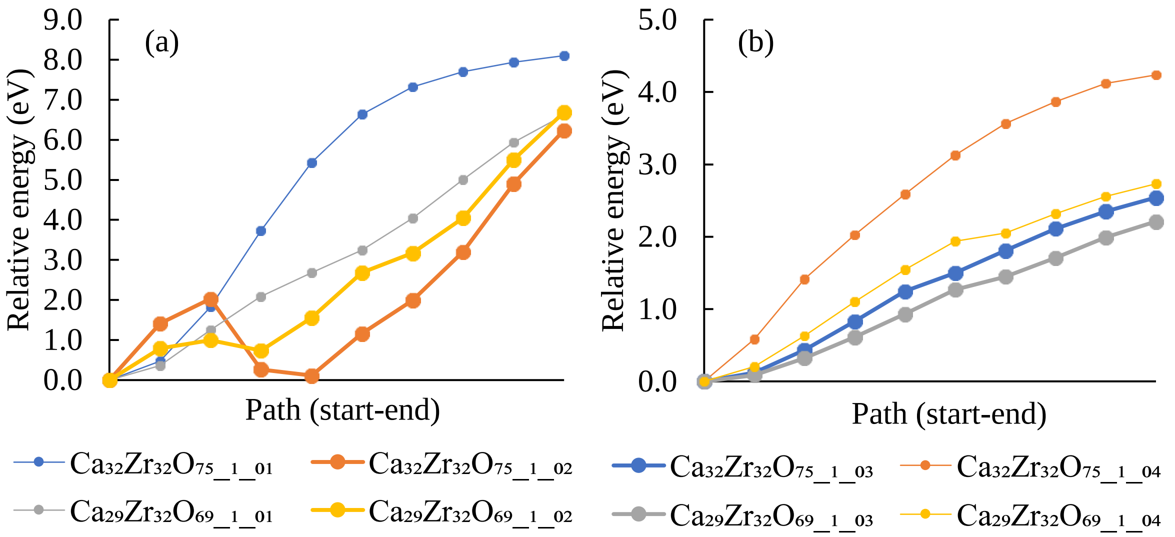

Figure S12. Energy profiles of atomic desorption from the defective (001) surface. (a) O paths, (b) Ca paths. Geometries of all paths are shown in the images in the following pages.

The images below display the migration of O/Ca/Zr atom(s), the energetics of which are shown in Figures S8-S12. The bright red/blue/green atoms enclosed by the black circles represent the migrating O/Ca/Zr atom(s). The left (a) and right (b) columns show the same path viewed from the side and top view, respectively.

○ $Ca_{12}Zr_{11}O_{28\_1\_01}$: O migration

(a)

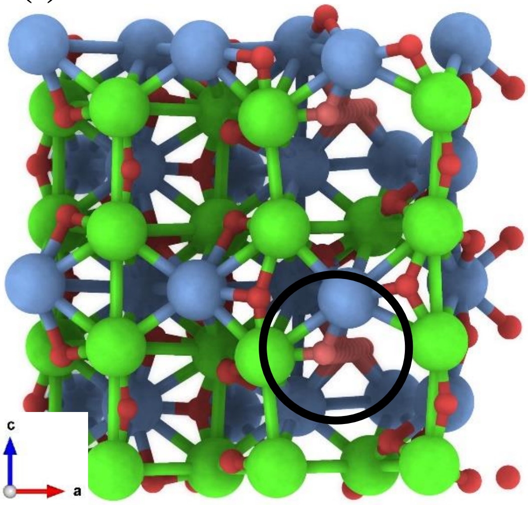

(b)

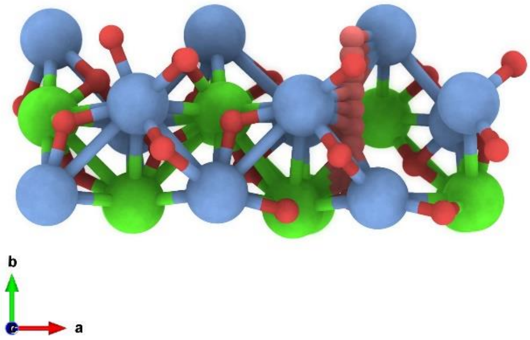

○ $Ca_{12}Zr_{11}O_{28\_1\_02}$: O migration

(a)

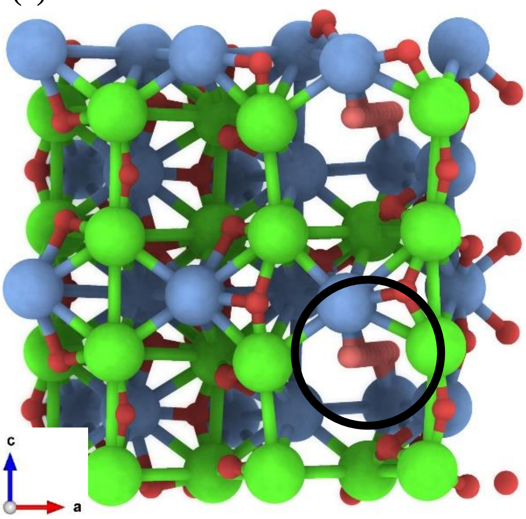

(b)

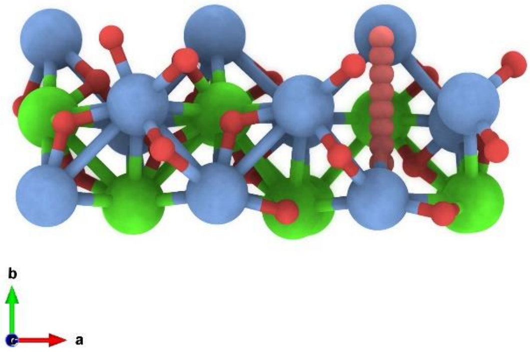

○ $Ca_{12}Zr_{11}O_{28\_1\_03}$: O migration

(a)

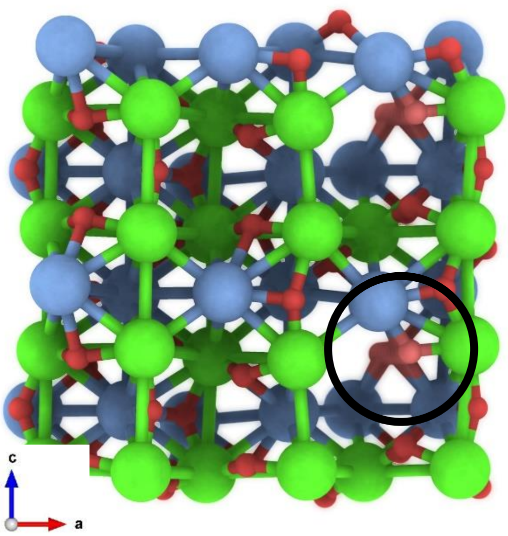

(b)

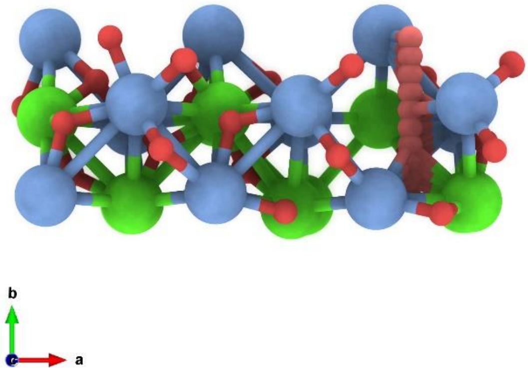

○ $Ca_{12}Zr_{11}O_{28\_1\_04}$: Ca migration

(a) (b)

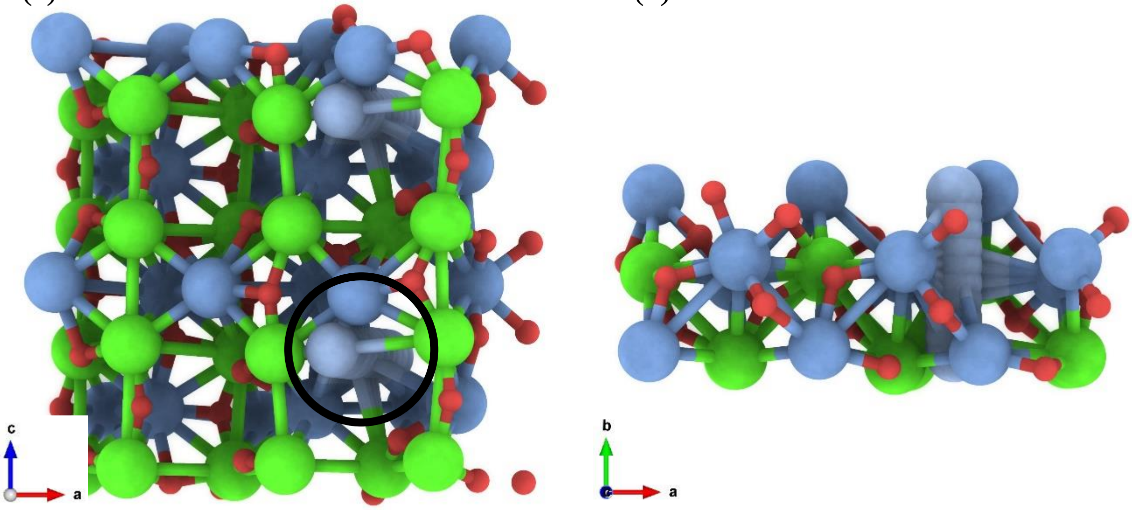

○ $Ca_{12}Zr_{11}O_{28\_1\_05}$: Ca migration

(a) (b)

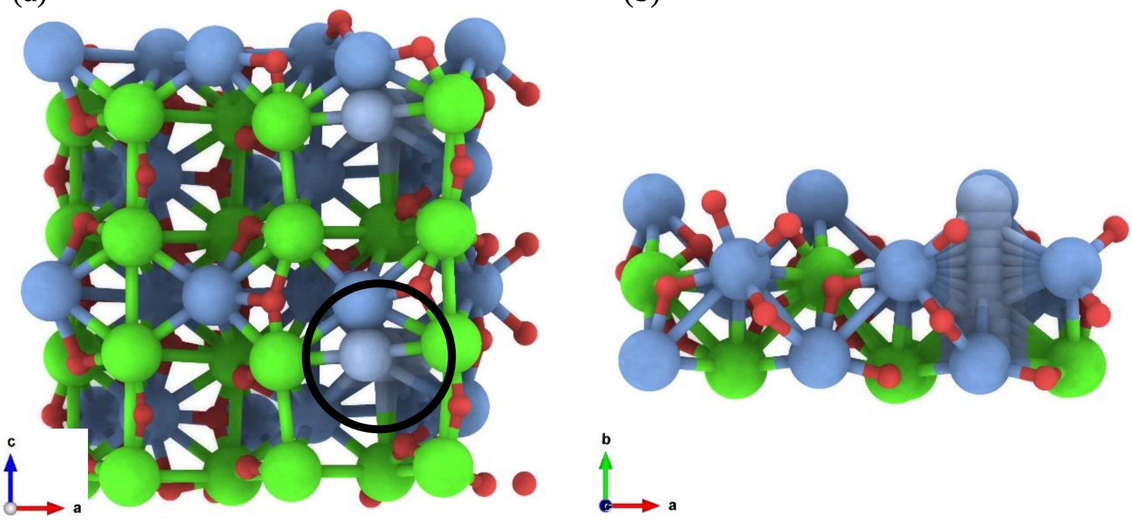

○ $Ca_{12}Zr_{11}O_{28\_1\_06}$: Ca migration

(a) (b)

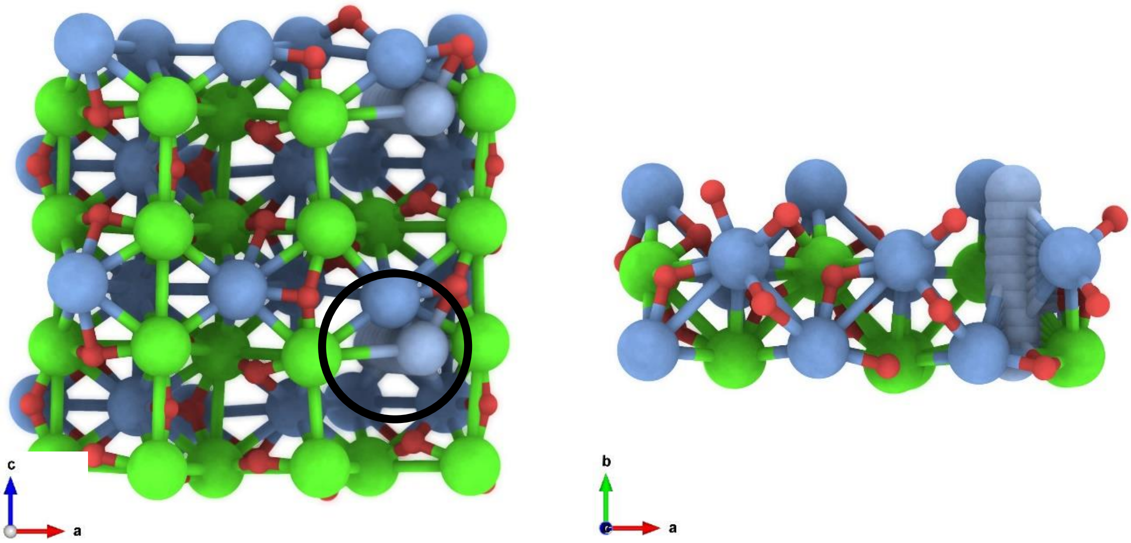

○ $Ca_{12}Zr_{11}O_{28\_1\_07}$: Ca migration

(a) 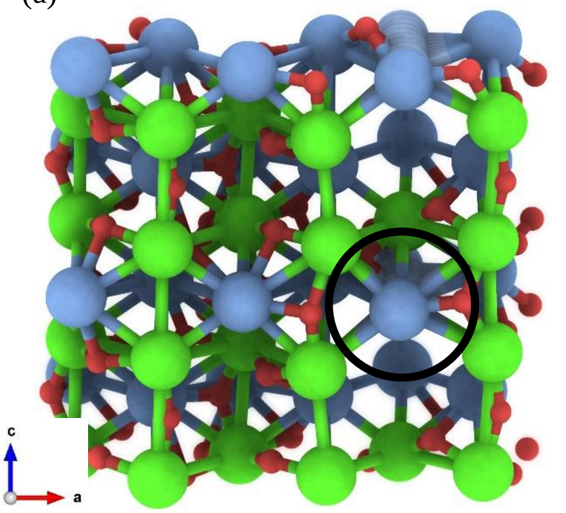

(b) 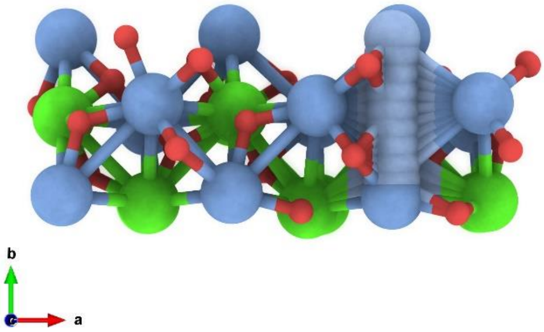

○ $Ca_{12}Zr_{11}O_{28\_1\_08}$: Ca migration

(a) 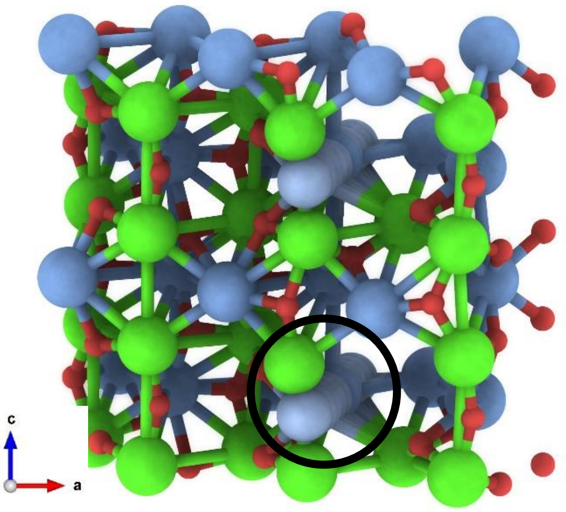

(b) 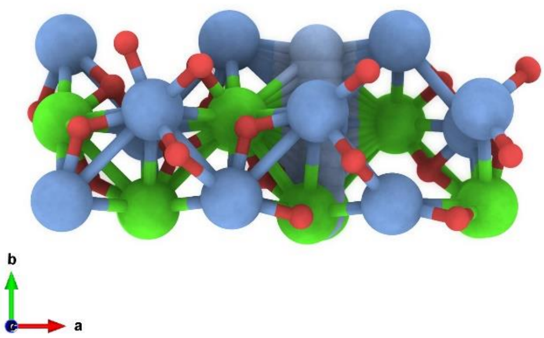

○ $Ca_{12}Zr_{11}O_{28\_1\_09}$: Ca migration

(a) 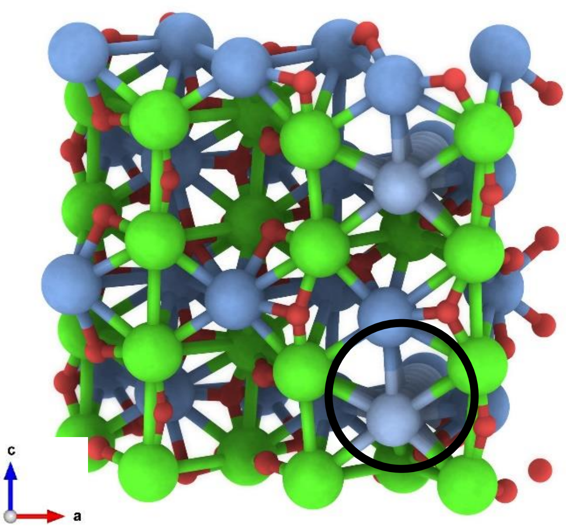

(b) 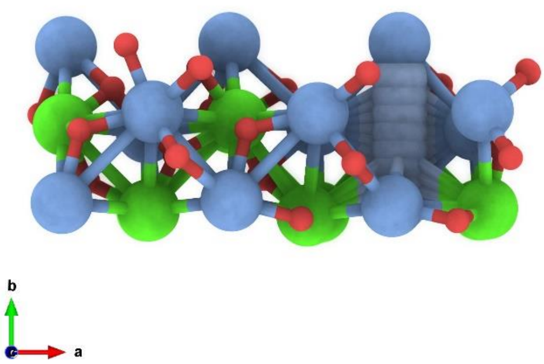

○ $Ca_{12}Zr_{10}O_{28\_1\_01}$: O migration

(a) (b)

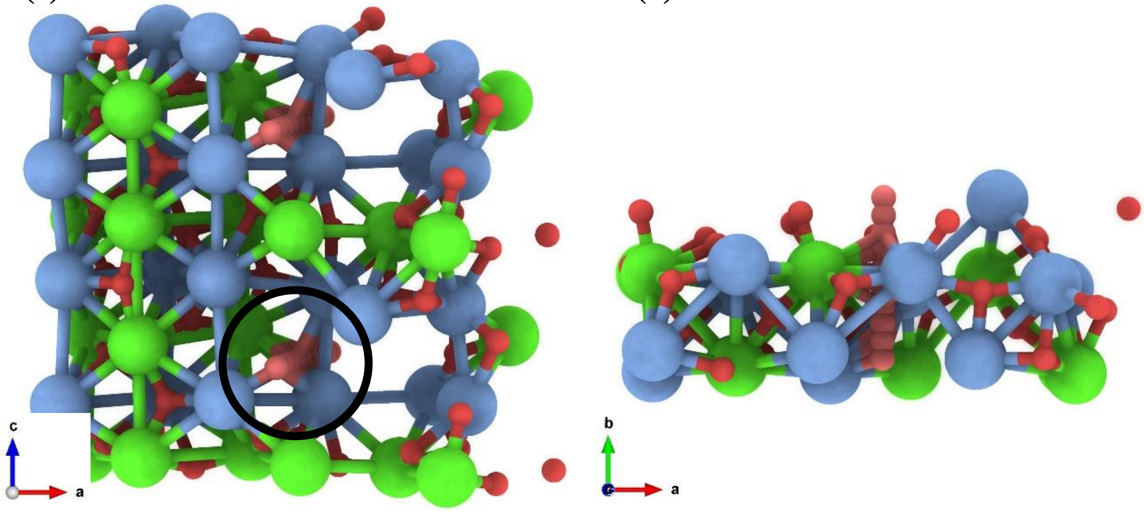

○ $Ca_{12}Zr_{10}O_{28\_1\_02}$: O migration

(a) (b)

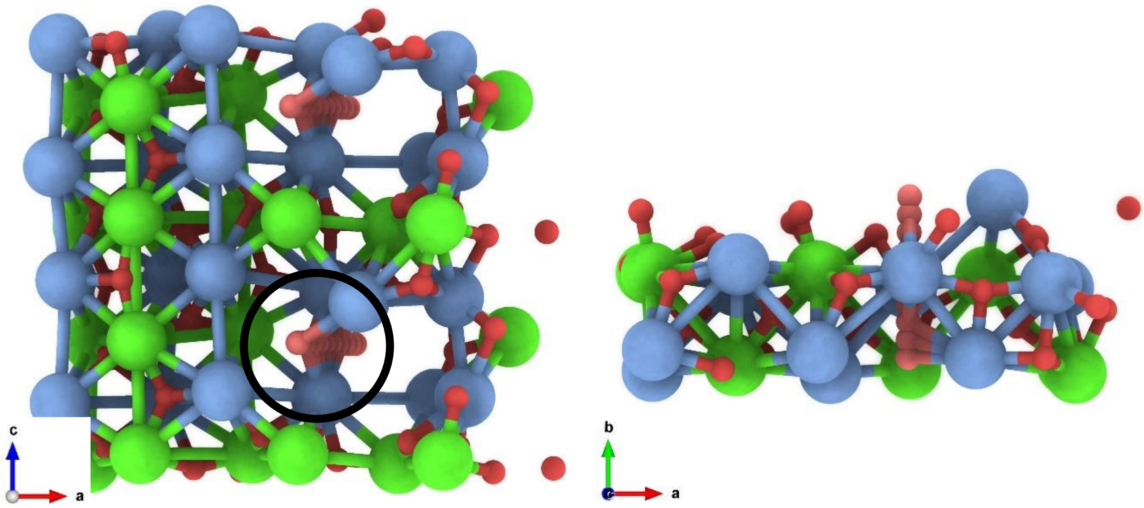

○ $Ca_{12}Zr_{10}O_{28\_1\_03}$: O migration

(a) (b)

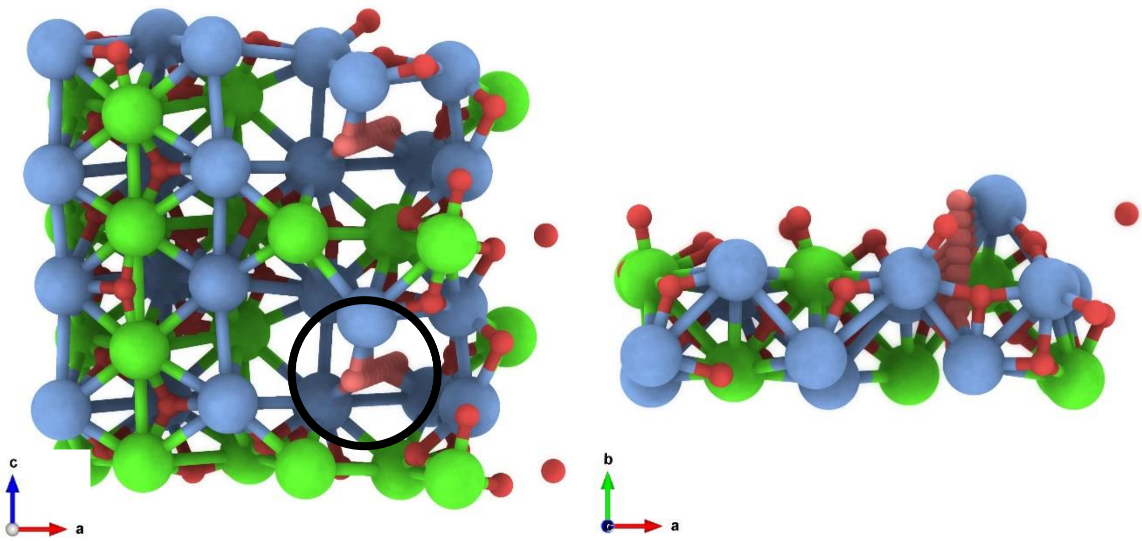

○ $Ca_{12}Zr_{10}O_{28\_1\_04}$: Ca migration

(a) (b)

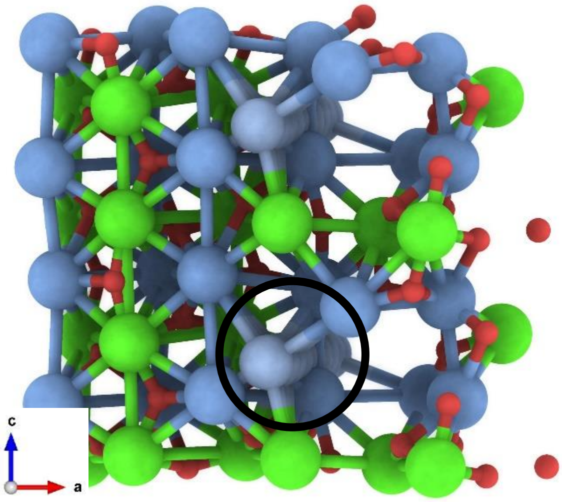

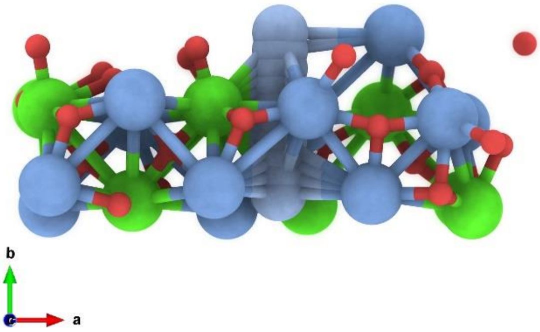

○ $Ca_{12}Zr_{10}O_{28\_1\_05}$: Ca migration

(a) (b)

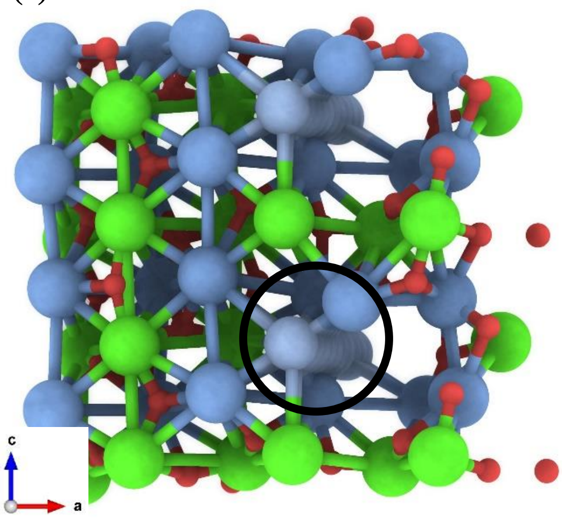

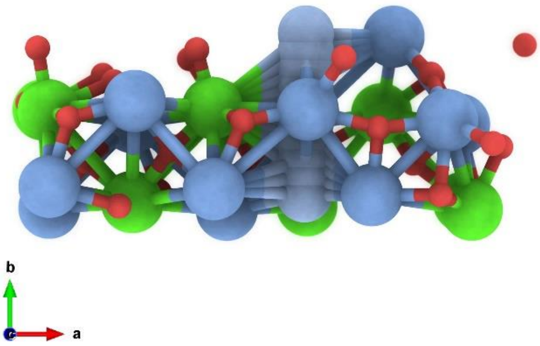

○ $Ca_{12}Zr_{10}O_{28\_1\_06}$: Ca migration

(a) (b)

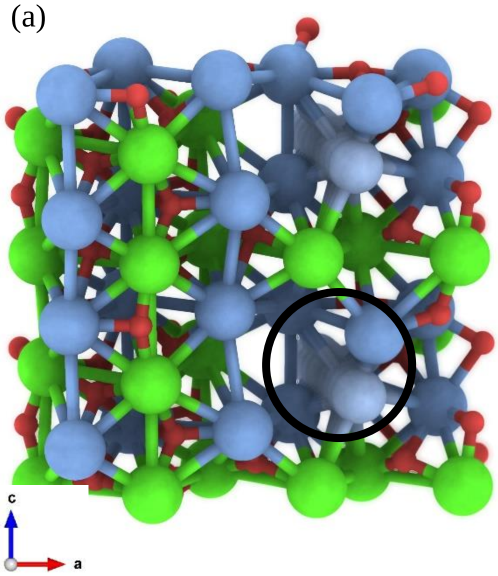

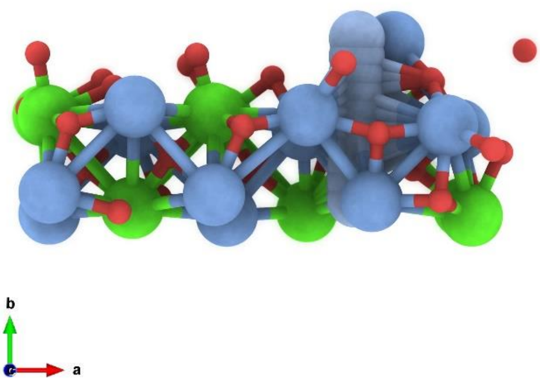

○ $Ca_{12}Zr_{10}O_{28\_1\_07}$: Ca migration

(a)

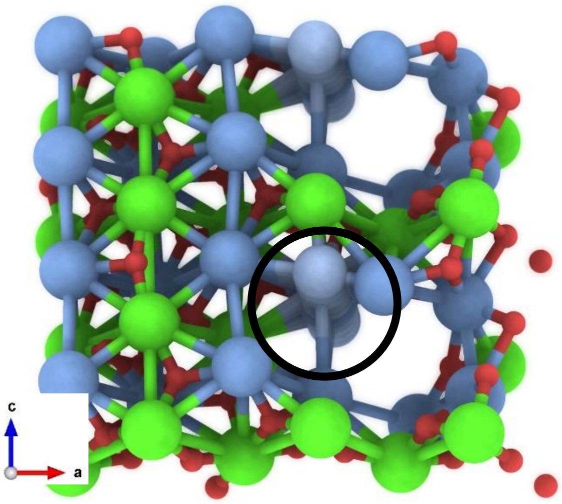

(b)

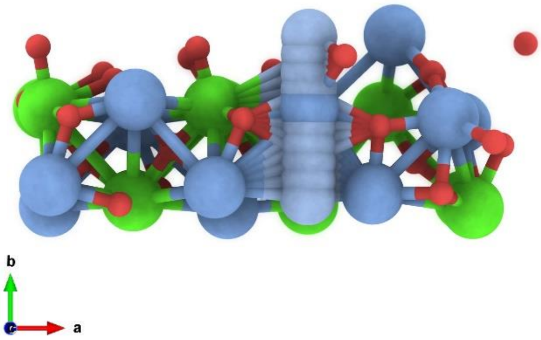

○ $Ca_{12}Zr_{10}O_{28\_1\_08}$: Ca migration

(a)

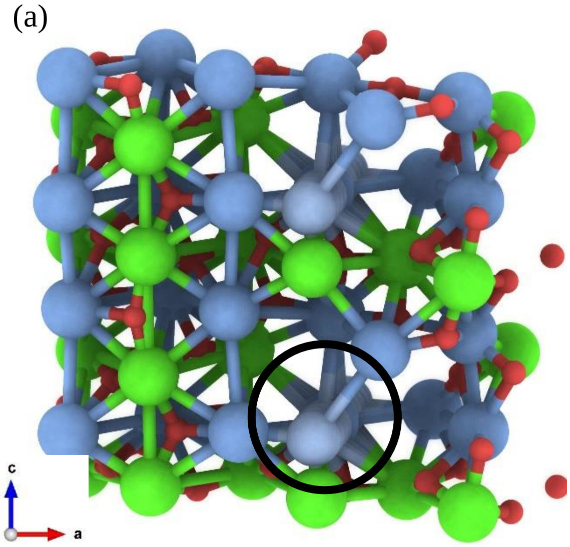

(b)

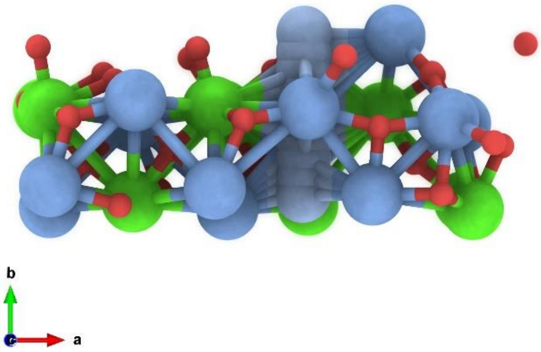

○ $Ca_{12}Zr_{10}O_{28\_1\_09}$: Ca migration

(a)

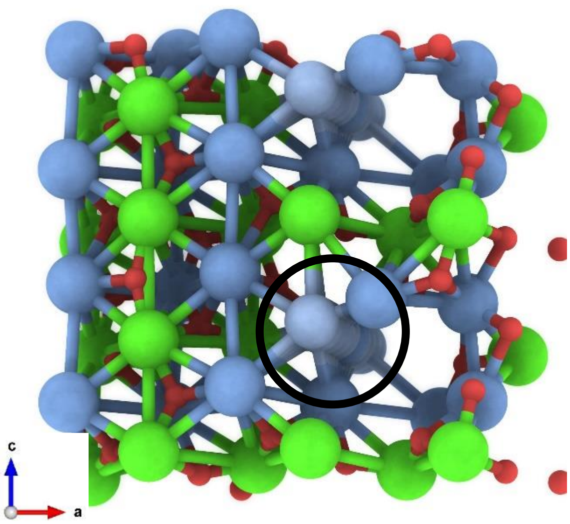

(b)

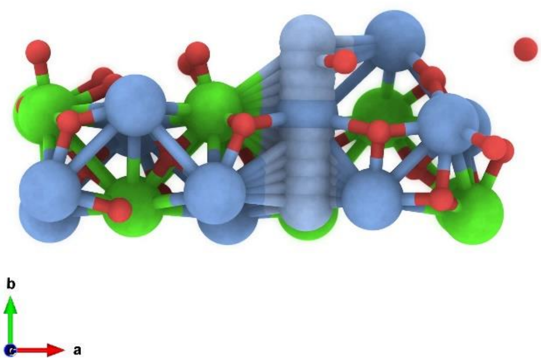

○ $Ca_{12}Zr_{10}O_{28\_1\_10}$: Ca migration

(a) (b)

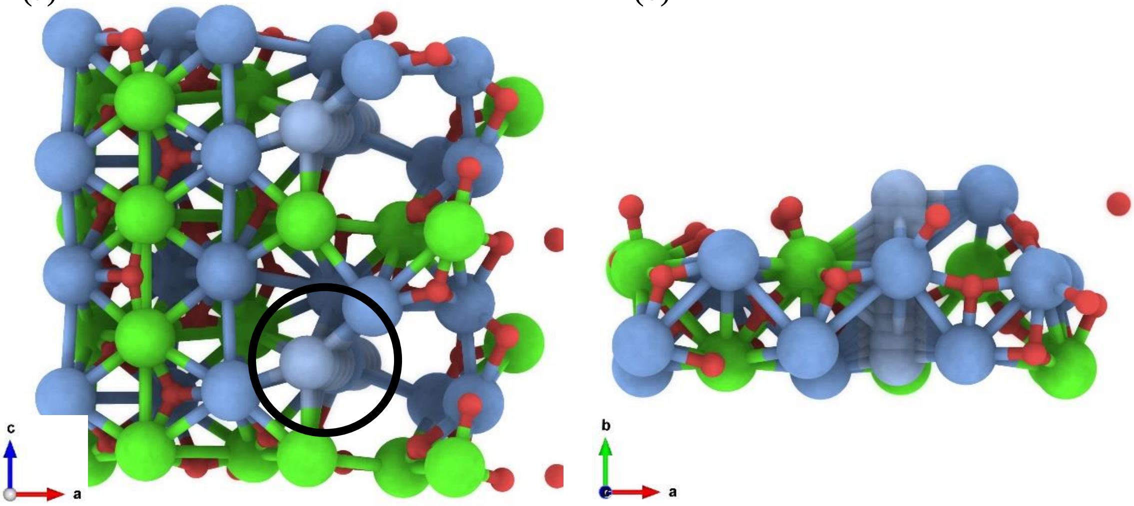

○ $Ca_{12}Zr_{12}O_{28\_1\_01}$: O migration

(a) (b)

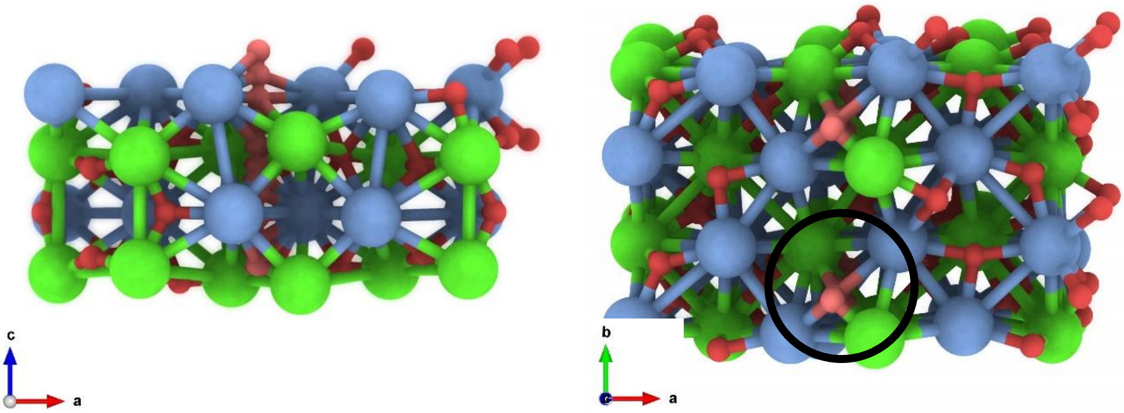

○ $Ca_{12}Zr_{12}O_{28\_1\_02}$: O migration

(a) (b)

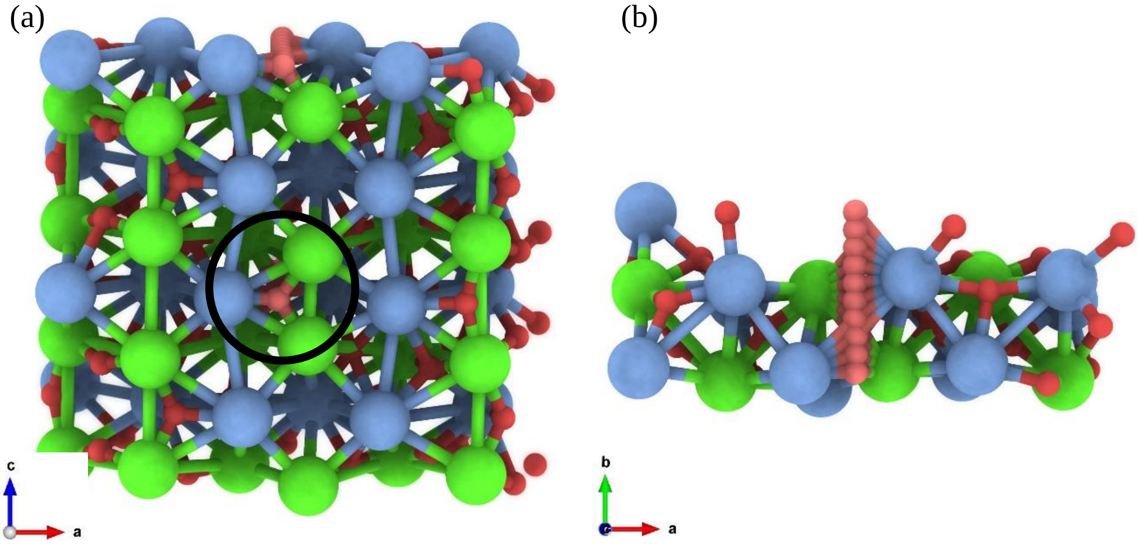

$Ca_{12}Zr_{12}O_{28\_1\_03}$: Ca migration

(a)

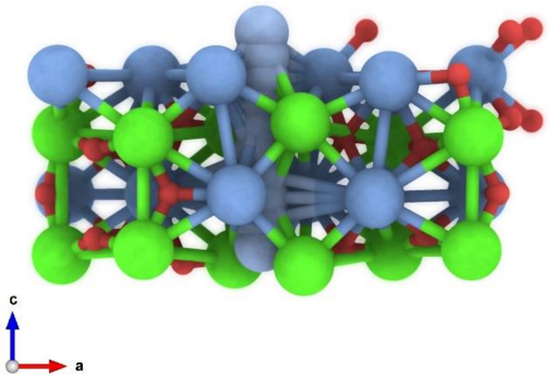

(b)

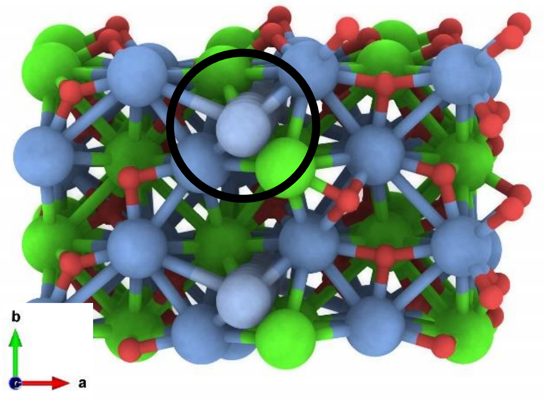

- $Ca_{12}Zr_{12}O_{28\_1\_04}$: Ca migration

(a)

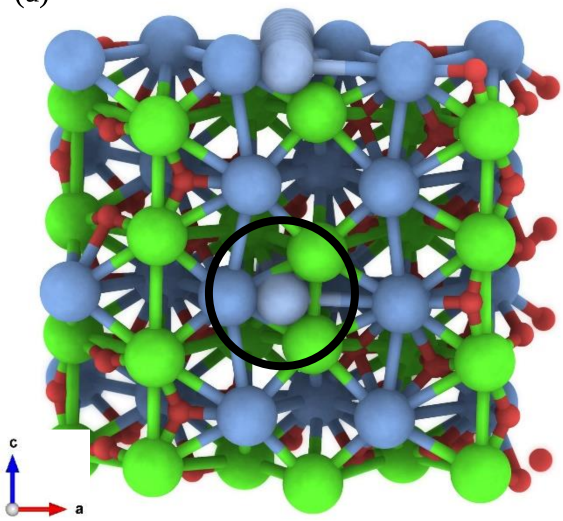

(b)

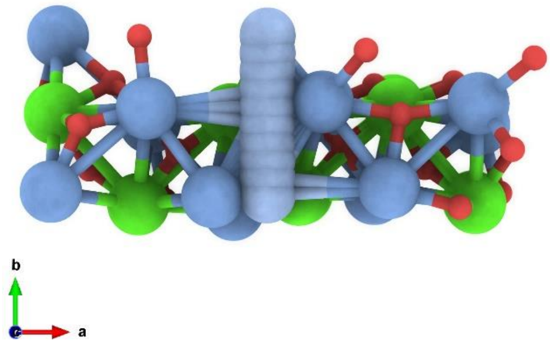

- $Ca_{12}Zr_{12}O_{28\_1\_05}$: Ca migration (2 atoms simultaneously)

(a)

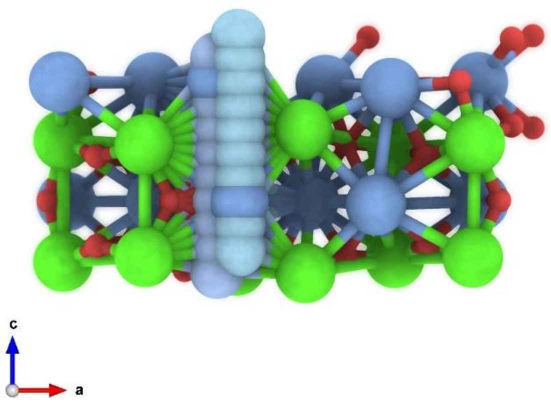

(b)

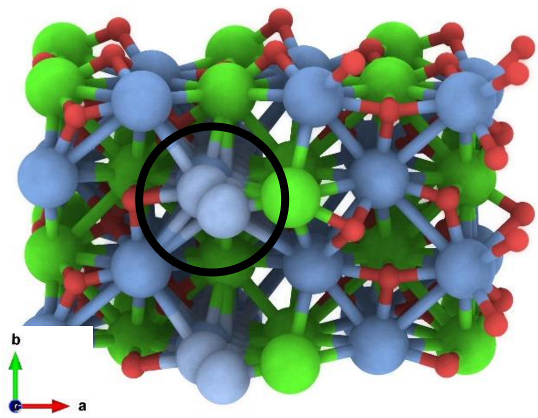

○ $Ca_{12}Zr_{12}O_{28\_1\_06}$: Ca migration (2 atoms simultaneously)

(a)

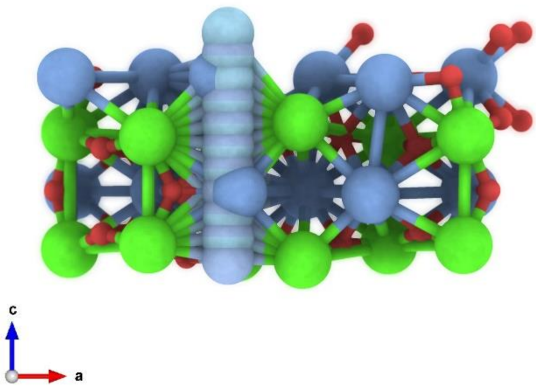

(b)

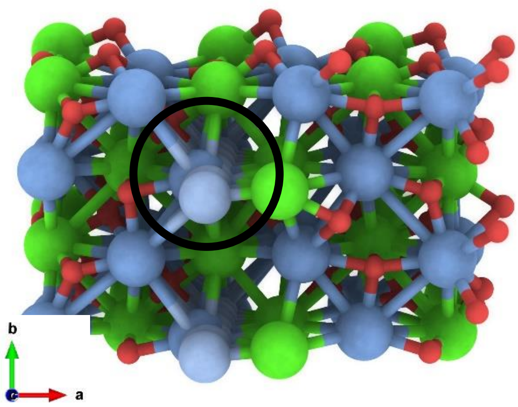

○ $Ca_{12}Zr_{12}O_{28\_1\_07}$: Ca migration (2 atoms simultaneously)

(a)

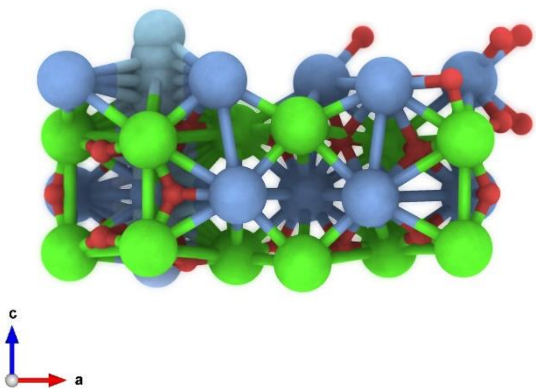

(b)

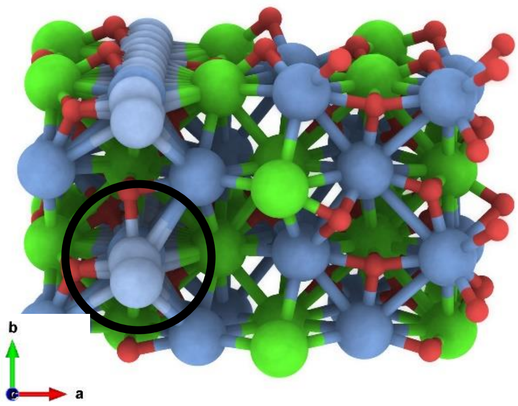

○ $Ca_{12}Zr_{12}O_{28\_1\_08}$: Ca migration (2 atoms simultaneously)

(a)

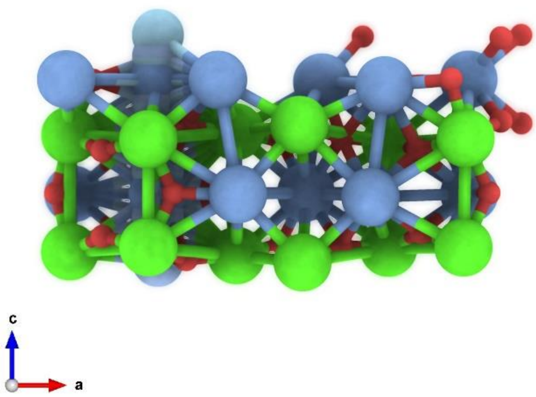

(b)

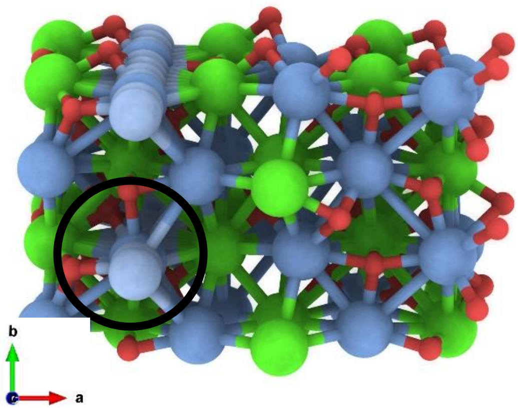

○ $Ca_{12}Zr_{12}O_{28\_1\_09}$: Zr migration (2 atoms simultaneously)

(a) (b)

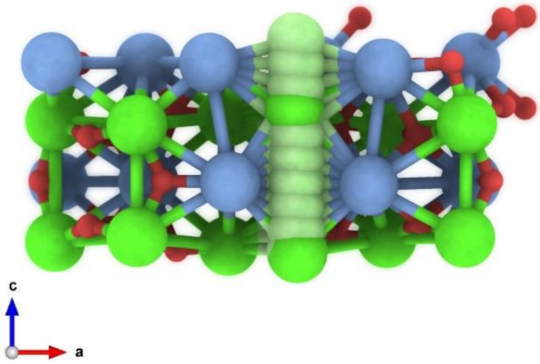

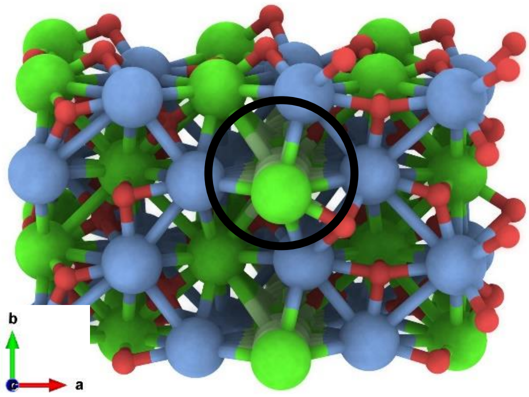

○ $Ca_{11}Zr_{12}O_{26\_1\_01}$: O migration

(a) (b)

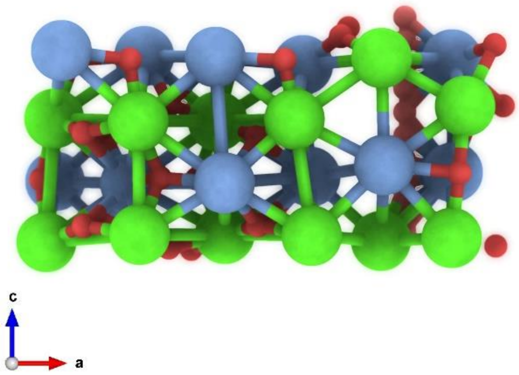

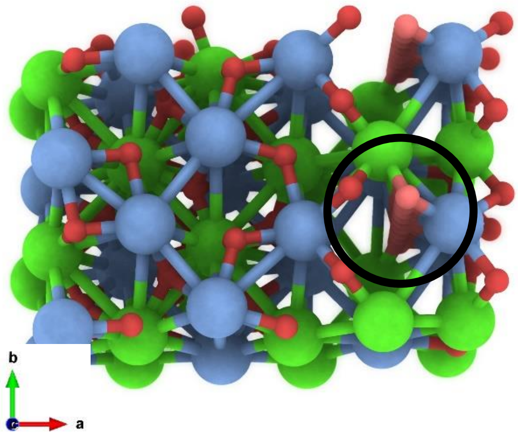

○ $Ca_{11}Zr_{12}O_{26\_1\_02}$: O migration

(a) (b)

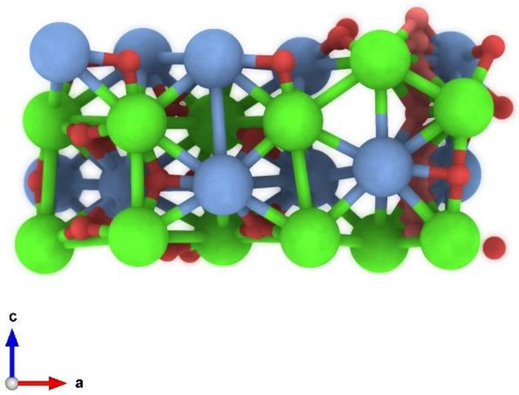

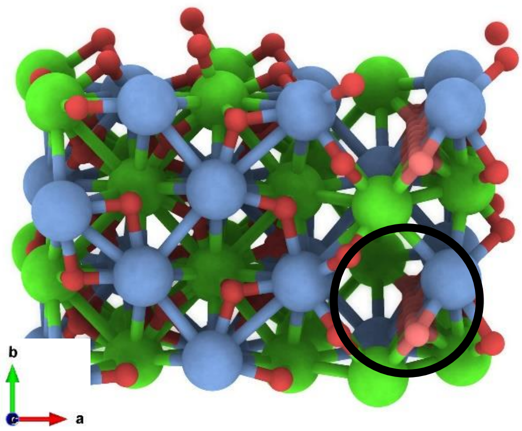

○ $Ca_{11}Zr_{12}O_{26\_1\_03}$: O migration

(a)

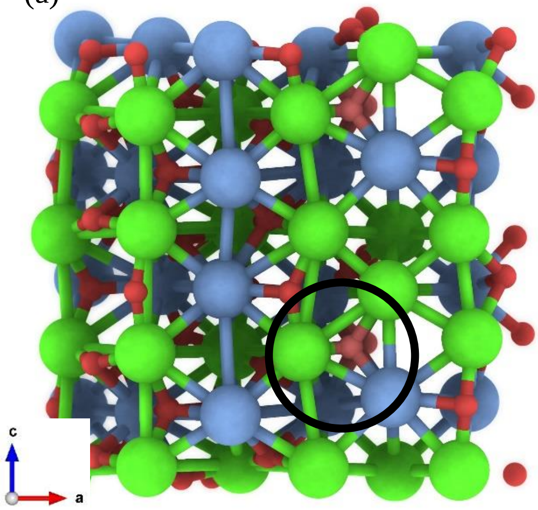

(b)

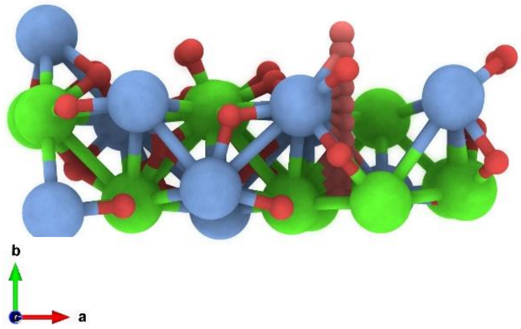

○ $Ca_{11}Zr_{12}O_{26\_1\_04}$: O migration

(a)

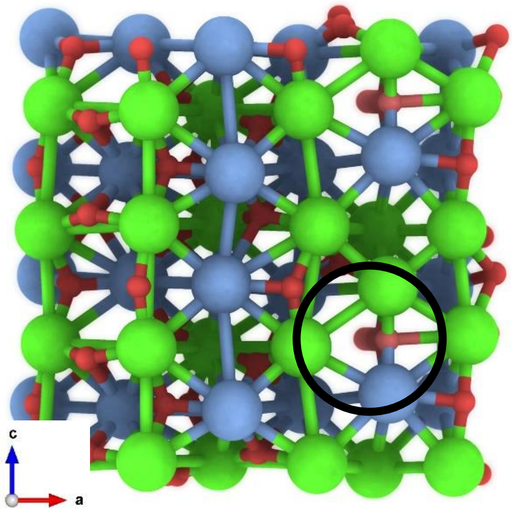

(b)

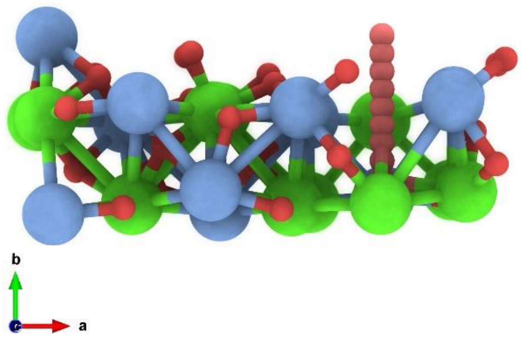

○ $Ca_{11}Zr_{12}O_{26\_1\_05}$: O migration

(a)

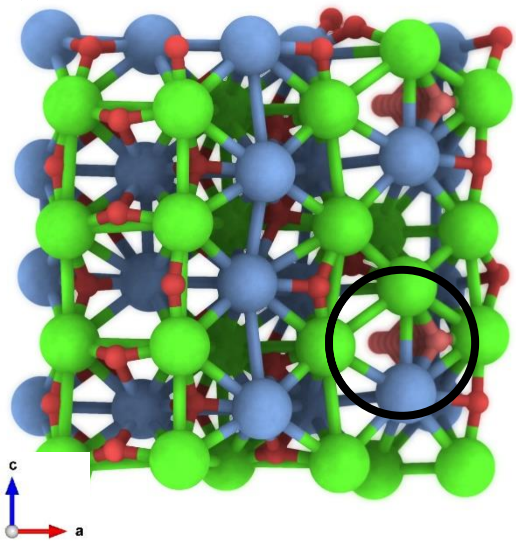

(b)

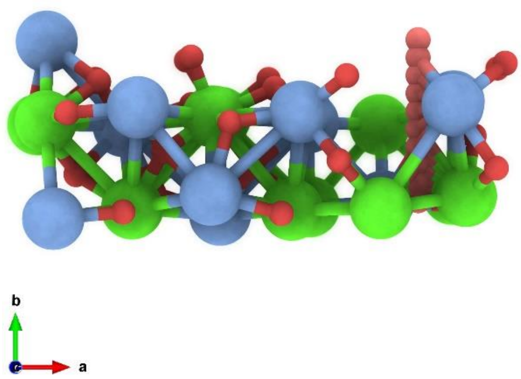

○ $Ca_{11}Zr_{12}O_{26\_1\_06}$: Ca migration

(a)

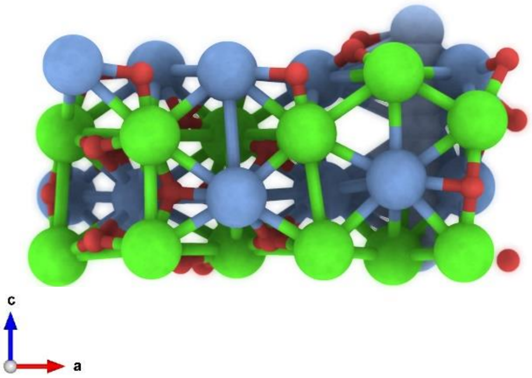

(b)

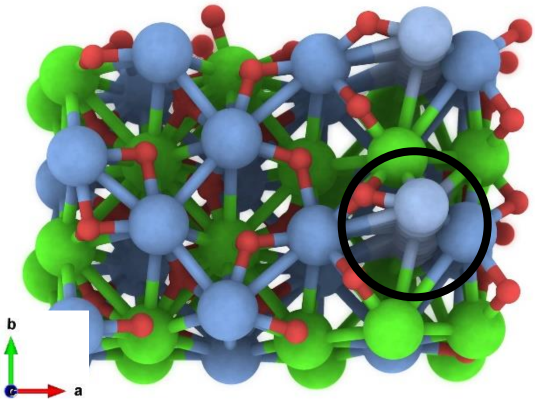

○ $Ca_{11}Zr_{12}O_{26\_1\_07}$: Ca migration

(a)

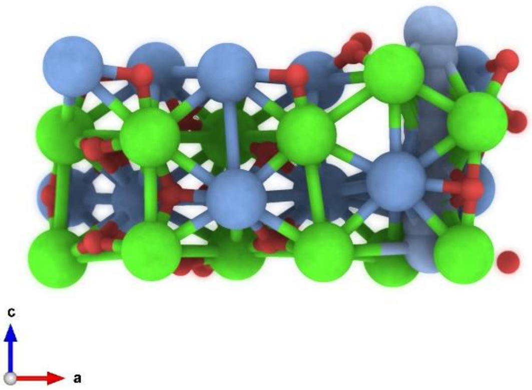

(b)

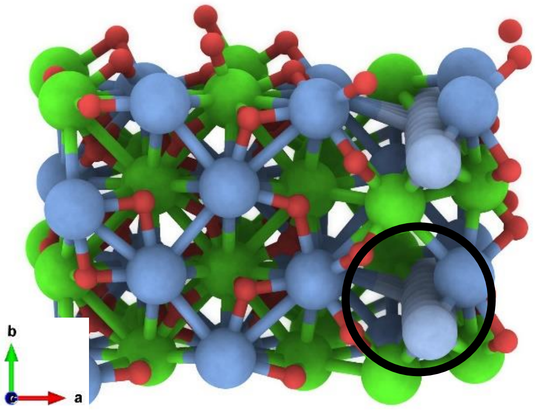

○ $Ca_{11}Zr_{12}O_{26\_1\_08}$: Ca migration

(a)

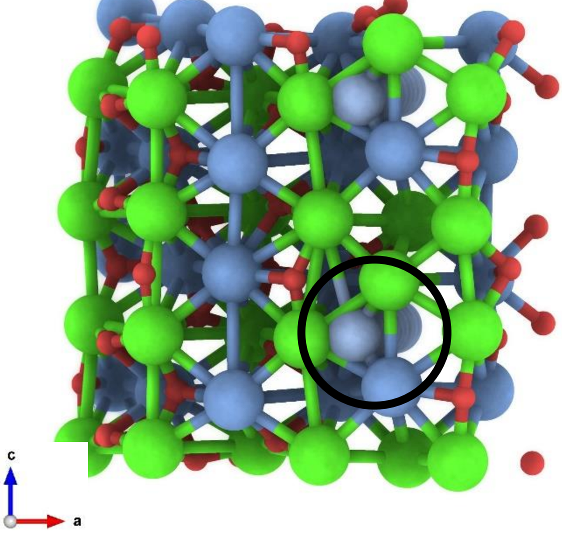

(b)

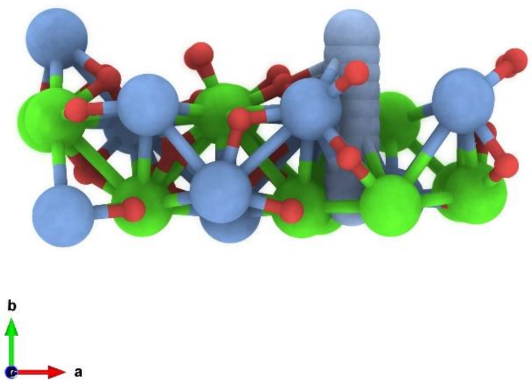

○ $Ca_{11}Zr_{12}O_{26\_1\_09}$: Ca migration

(a)

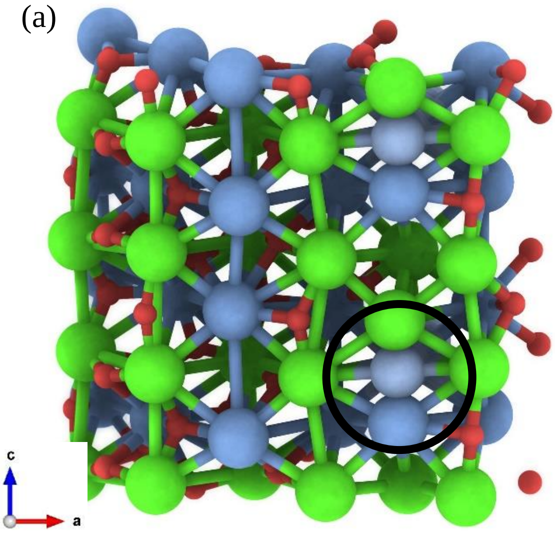

(b)

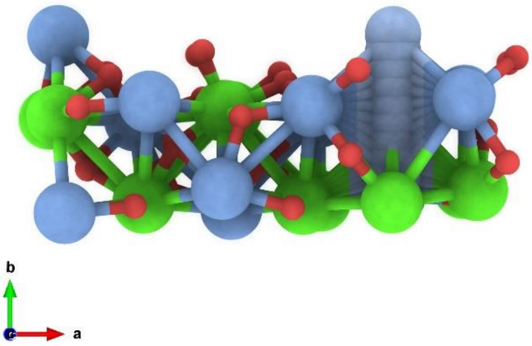

○ $Ca_{11}Zr_{12}O_{26\_1\_10}$: Ca migration

(a)

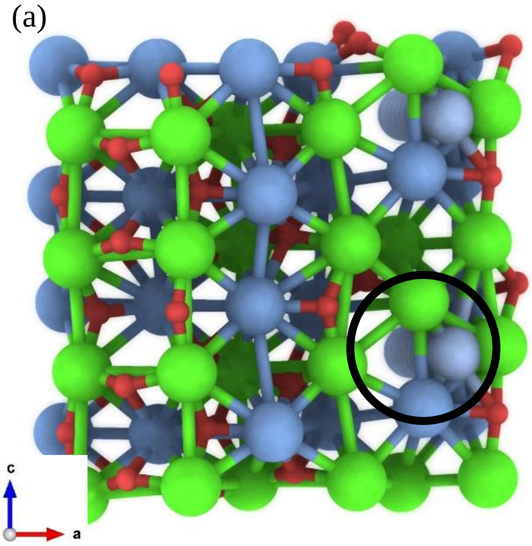

(b)

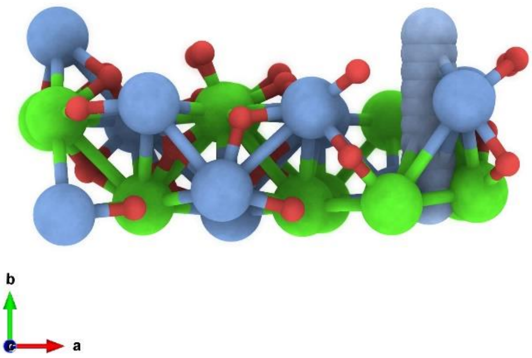

○ $Ca_{11}Zr_{12}O_{26\_1\_11}$: Ca migration

(a)

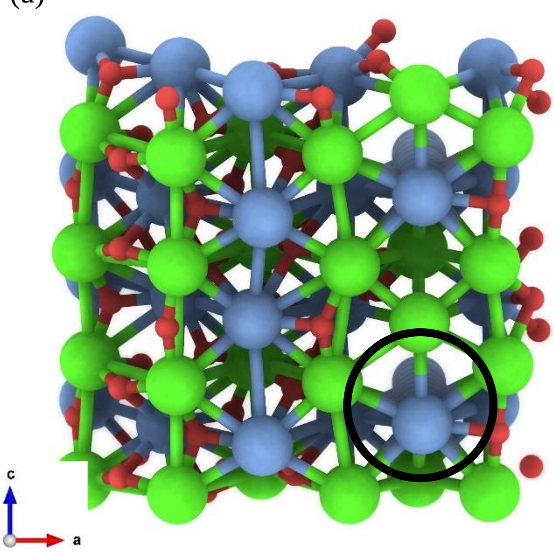

(b)

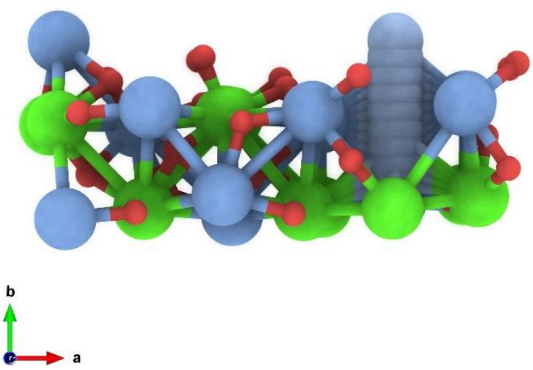

○ $Ca_{11}Zr_{12}O_{26\_1\_12}$: Ca migration

(a)

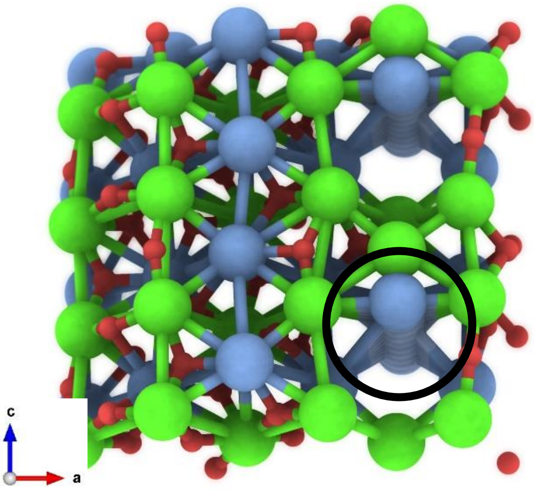

(b)

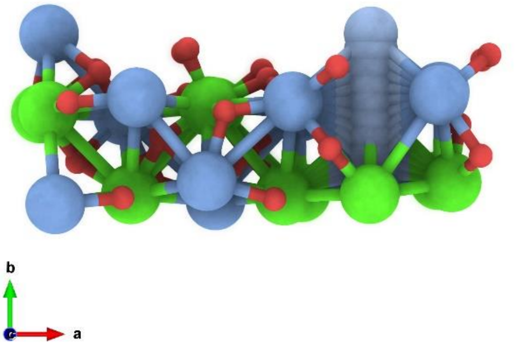

○ $Ca_{11}Zr_{12}O_{26\_1\_13}$: Ca migration (2 atoms simultaneously)

(a)

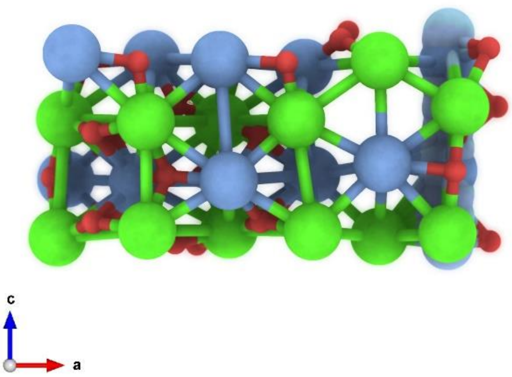

(b)

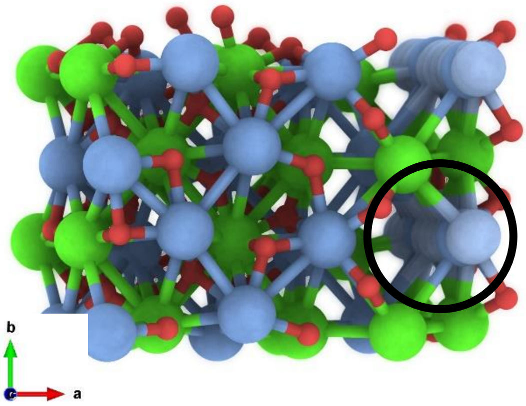

○ $Ca_{11}Zr_{12}O_{26\_1\_14}$: Ca migration (2 atoms simultaneously)

(a)

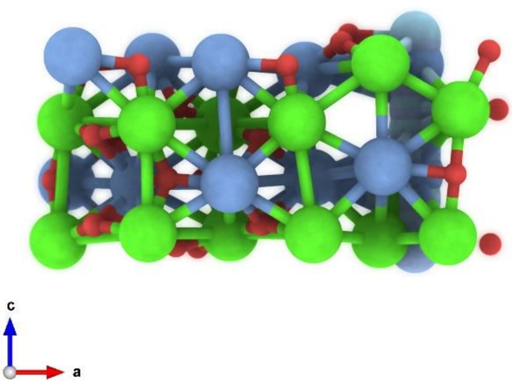

(b)

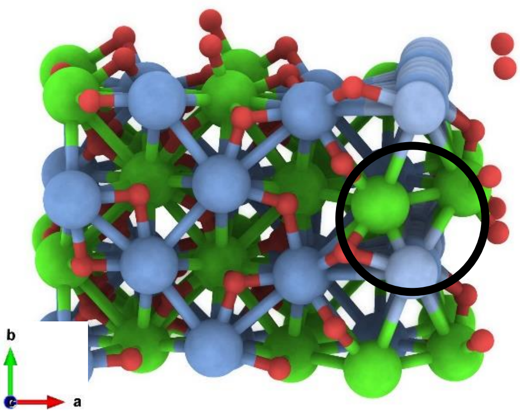

○ $Ca_{11}Zr_{12}O_{26\_1\_15}$: Zr migration

(a)

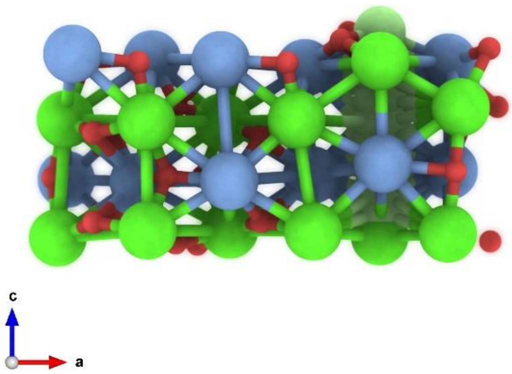

(b)

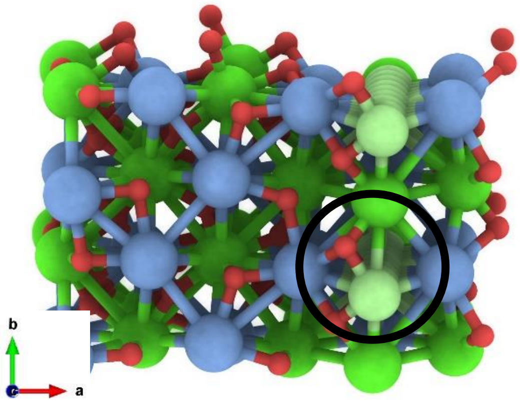

○ $Ca_{32}Zr_{32}O_{75\_1\_01}$: O desorption

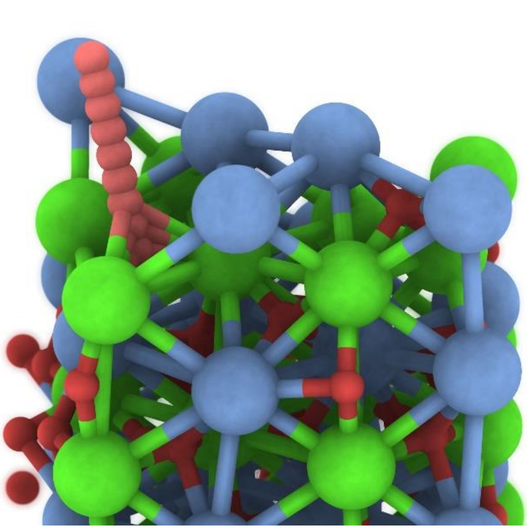

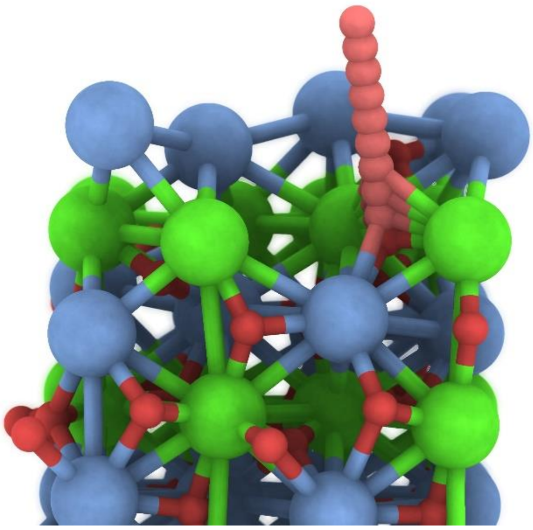

○ $Ca_{32}Zr_{32}O_{75\_1\_02}$: O desorption

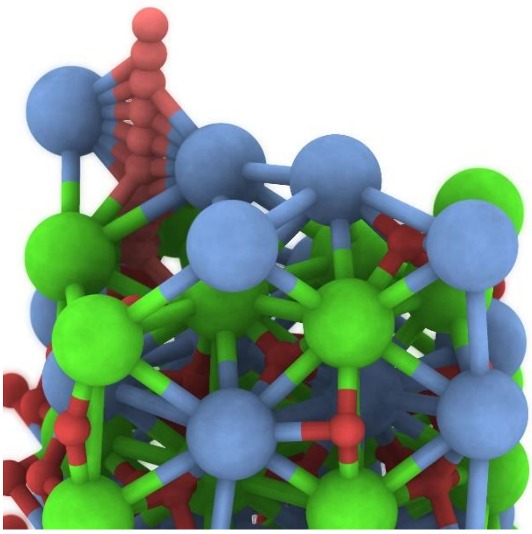

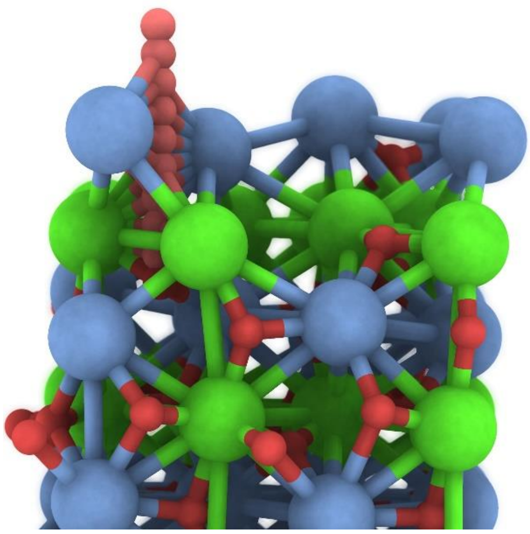

○ $Ca_{32}Zr_{32}O_{75\_1\_03}$: Ca desorption

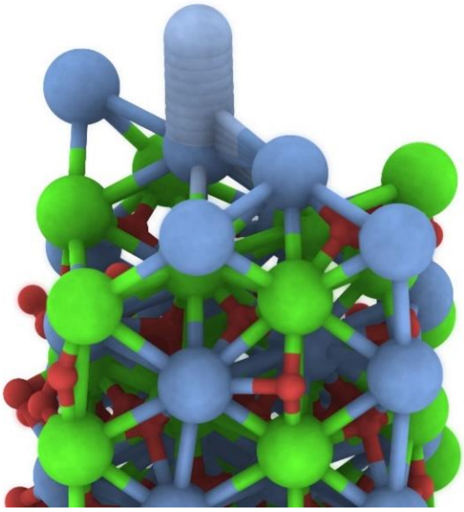

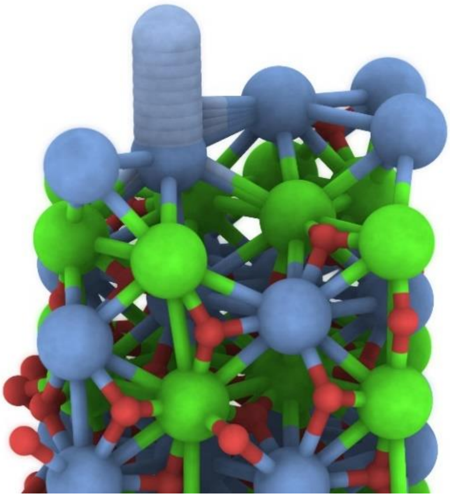

○ $Ca_{32}Zr_{32}O_{75\_1\_04}$: Ca desorption

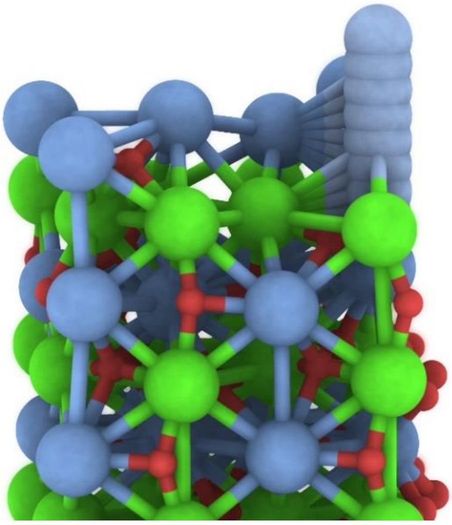

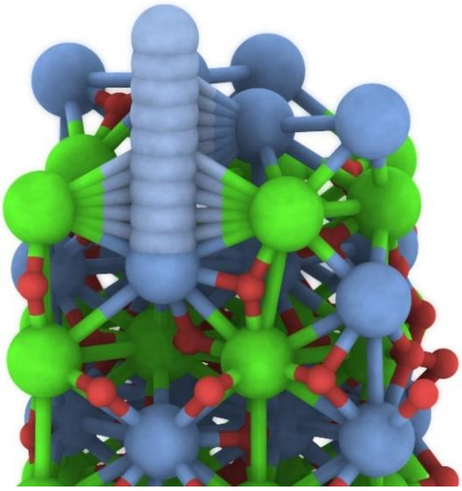

○ $Ca_{29}Zr_{32}O_{69\_1\_01}$: O desorption

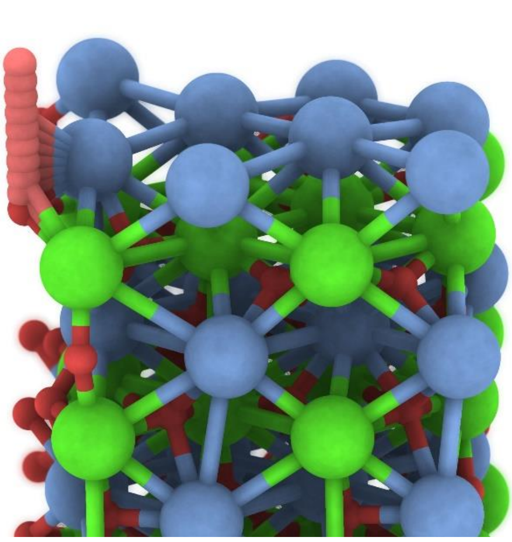

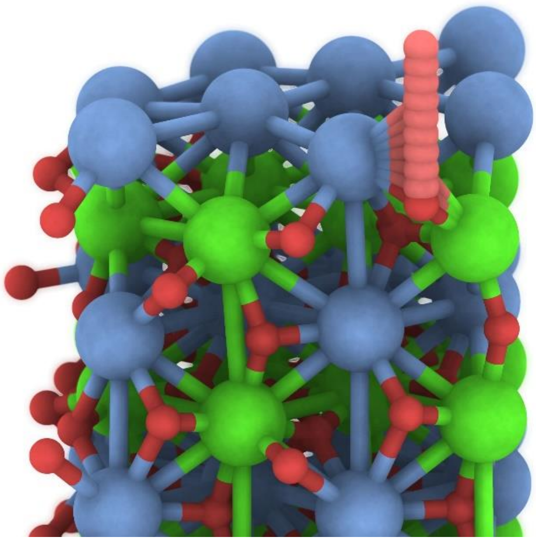

- $Ca_{29}Zr_{32}O_{69\_1\_02}$: O desorption

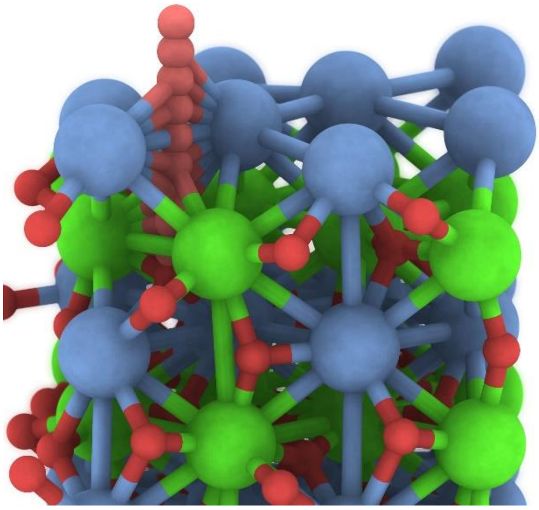
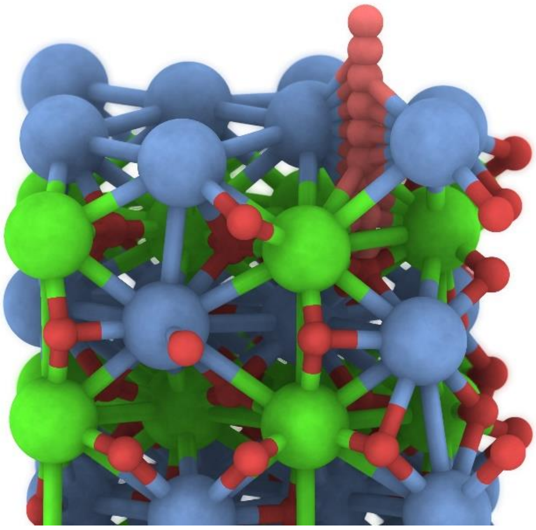

- $Ca_{29}Zr_{32}O_{69\_1\_03}$: Ca desorption

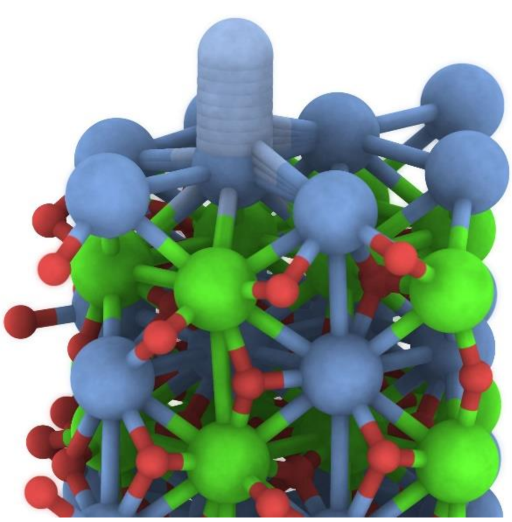
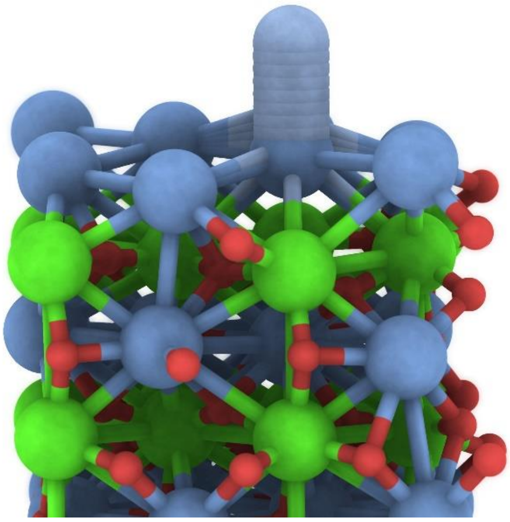

- $Ca_{29}Zr_{32}O_{69\_1\_04}$: Ca desorption

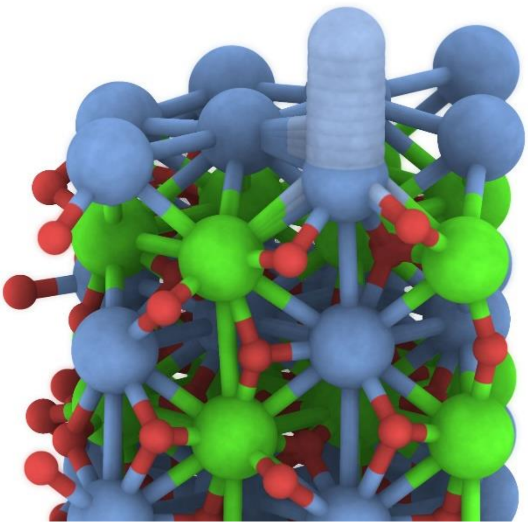
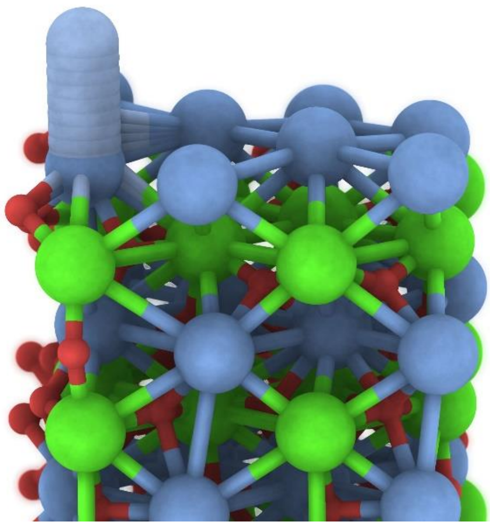

References

1. M. G. Brik, C. -G. Ma, V. Krasnenko, *Surface Science* 2013, **608**, 146–153. https://doi.org/10.1016/j.susc.2012.10.004.